Available online at www.sciencedirect.com
SCIENCE DIRECT®
Sedimentary Geology 161 (2003) 309–337
Sedimentary Geology
www.elsevier.com/locate/sedgeo

Sedimentary signatures and processes during marine bolide impacts: a review

Henning Dypvik[a,*], Lubomir F. Jansa[b]

[a] Department of Geology, University of Oslo, P.O. Box 1047, Blindern, N0316 Oslo, Norway
[b] Geological Survey of Canada-Atlantic, P.O. Box 1006, Dartmouth, NS, Canada B2Y4A2

Received 9 April 2001; accepted 28 March 2003

Abstract

Studies of submarine impact craters resulting from impacts of comets or asteroids demonstrate that the presence of water and the physical properties of target rocks have a major influence on sedimentary processes associated with meteorite impacts. This results in difference in sedimentary signature of bolide impacts in marine environments compared to subaerial impact craters. In subaerial impacts, the targets are commonly hard rocks, frequently of igneous and/or metamorphic origin, whereas in submarine impacts, the targets are mostly unconsolidated or poorly lithified sediments, or sedimentary rocks, with high volumes of pore water. Such differences result in variability in crater morphology and in sedimentary processes inside and outside the impact area.

Impacts in shallow-water marine (neritic) environments produced craters with low or absent rims and wide and shallow brims, as characterize by both the Montagnais (on the Scotian shelf), the Mjølnir (in the Barents Sea), 45 and 40 km in diameter, respectively, and the Chesapeake Bay (90 km in diameter). Lack of elevated rims is thought to be the result of current reworking and resurge of the water back into the excavated cavity, as the water in the crater is vaporized. During this process, resurge gullies can be cut across the rim, while mass- and debris-flows, turbidites, and other gravity deposits are produced as results of tsunami and crater-wall and central high collapse, during and after the crater excavation stage. Such deposits are found both within and outside the crater structure.

The only difference between gravity deposits triggered by an impact or other rare events, such as earthquakes, is the admixture of various melt particles and possible enrichments in iridium in the former.

Impacts near the shelf edge may cause partial collapse of the continental margin as shown by the Montagnais and Chicxulub impacts. Some of the gravity and debris flows generated by margin collapse may be channelized, with final deposits up to several hundred meters thick, extending for hundreds of kilometers from the impact site. Other impact features such as shatter cones, tektites, spherules and Ni-spinels, shocked quartz, isotropication, and partial melts, are common to both submarine and subaerial impacts.

Theoretical calculations of the destructive forces of mega-tsunami waves triggered by meteorite impact in the ocean greatly exceed those based on geologic evidence. A dearth of gigantic tsunami evidence for the Chicxulub impact outside of the Gulf of Mexico, where from theoretical modelling the maximum near bottom orbital velocity of water flow crossing the deep North Atlantic basin should have been >1 m/s, could be the result of the mitigating effect of the bathymetry of surrounding area, causing wave diffraction and interference. Calculated maximum horizontal orbital velocity near the seafloor at the shelf for the Montagnais impact is 22 m/s for a 200-m-high wave, 5.5 m/s for a 50-m-high wave at 500 km, decreasing to 0.5 m/s at 1000

* Corresponding author. Fax: +47-22-85-42-15.
E-mail addresses: henning.dypvik@geologi.uio.no (H. Dypvik), jansa@agc.bio.ns.ca (L.F. Jansa).

doi:10.1016/S0037-0738(03)00135-0

km, strong enough to scour the deep ocean bottom and produce distinct erosion surfaces and disconformities in marine sedimentary record. However, lack of cores across impact horizon prevents confirmation of occurrence of such bottom water flows.

Keywords: Montagnais; Mjølnir; Submarine craters; Sedimentary processes; Mega-tsunami

1.. Introduction

1.1. General background

A total of 170 meteorite impact craters (and ejecta) have been found/confirmed on the Earth's surface (Fig. 1) (Abels et al., 2002; Grieve et al., 1995; Gersonde et al., 2002; Whitehead, 2002). Seven of these remained located in the marine environment, while 20 originally marine impacts are presently located on land (Table 1) as a result of subsequent geologic processes. The submarine impact craters represent ~20% of global craters known, values much too low given that more than 70% of the Earth is covered by water. Glikson (1999) estimated that 8104 oceanic craters larger than 20 km should have formed during the last 3.5 Ga, a large number compared to the 27 craters and ejecta presently confirmed. This discrepancy is mainly due to plate tectonic destruction processes, lack of detailed data on morphology and sub-bottom characteristics of deep oceanic basins, and long-term erosional processes on the continents.

Impact cratering processes have been extensively studied on planetary surfaces and in particular at subaerial craters on the Earth. A thorough treatment of the physics of impact cratering is given by Melosh (1989), with an overview of the cratering processes on Earth published by Sharpton and Grieve (1990), Grieve (1998), Grieve et al. (1995), French (1998)

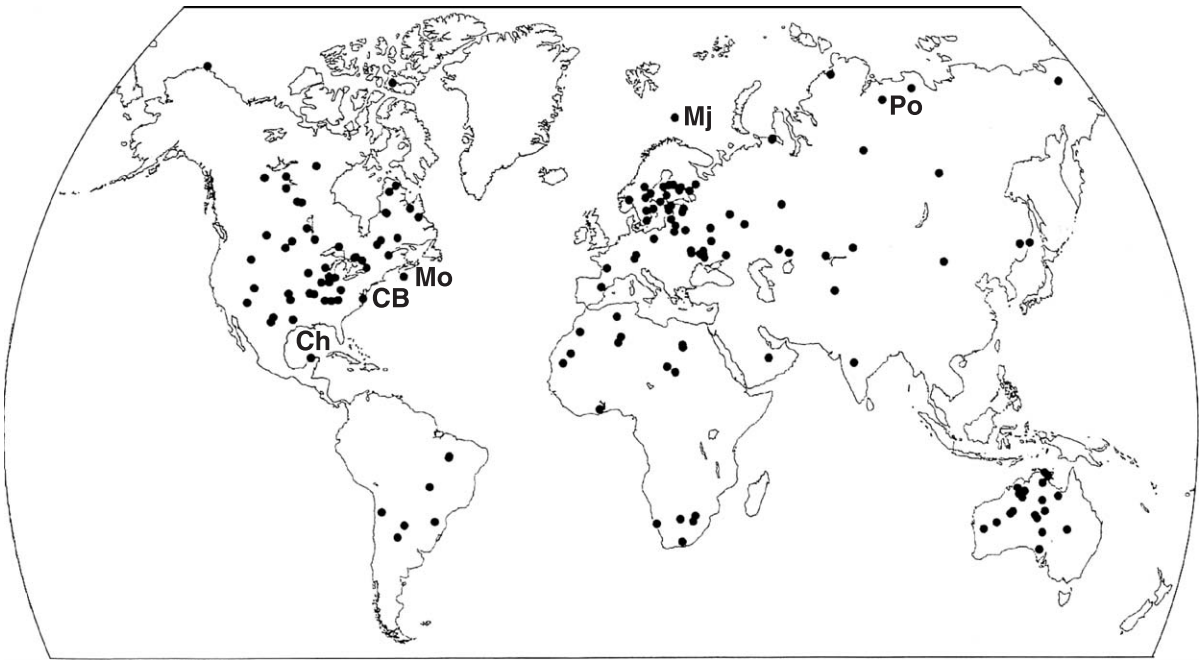

Fig. 1. World map showing locations of impact craters (modified from Grieve, 1998; with Chicxulub (Ch), Chesapeake Bay (CB), Mjølnir (Mj), Montagnais (Mo) submarine craters and Popigai (Po) highlighted).

Table 1
Submarine impact craters and bathypelagic impacts

Crater	Locality	Age (million years)	Diameter	Water depth at impact
(A) Submarine craters (craters formed and remain located in the sea/ocean)				
Chesapeak Bay	Virginia, USA	35.5 ± 0.3	90	200–500
Mjølnir	Barents Sea, Norway	142 ± 2.6	40	200–400
Montagnais	Nova Scotia, Canada	50.5 ± 0.76	45	112
Neugrund	Gulf of Finland, Estonia	535	20	50
Ust Kara	Kara Sea, Russia	70.3 ± 2.2	25	30–200
Bathypelagic-ejecta				
Eltanin	South Pacific	2 to 15	?	4700
(B) Marine impacts (craters presently exposed on land/subaerial)				
Avak	Alaska, USA	>95	12	<100 m
Chicxulub	Yucatan, Mexico	64.98 ± 0.05	170–310	<50
Gusev	Donets, Russia	49.0 ± 0.2	3	150–200
Granby	Linköping, Sweden	470	3	50–100
Kaluga	Kaluga, Russia	380 ± 5	15	100–800
Kamensk	Donets, Russia	49 ± 0.2	25	150–200
Kara	Kara Sea, Russia	70.3 ± 2.2	65	30–200
Kärdla	Hiiumaa, Estonia	455	4	20
Karikkoselkä	Läsi-Suomi Finland	440–450	1.3	? shallow water
Lockne	Östersund, Sweden	>455	13.5	>200
Wetumpka	Alabama, USA	81.0 ± 1.5	7.6	35–100
Possible marine impacts				
Gardnos	Hallingdal, Norway	650–700	5	? shallow water
Lumparn	Åland, Finland	440–460	9	? shallow water
Tvären	Tvären Bay, Sweden	>455	2	100–150
Marine ejecta				
Wittenoom Formation	Hamersley, V. Australia	2541	?	200
Eltanin	South Pacific	2 to 15	?	4700
Suggested marine impact craters/structures/related deposits				
Mulkarra	Eromanga, Australia	105	20	? shallow water
Skiyli	Western Kazakhstan	45 ± 5	3.2	300
Alamo breccia	Alamo, NV, USA	Frasnian (370)	?	?
Ragozinka	Middle Ural, Russia	Eocene, 46 ± 3	9	?

Basic data from Abels et al. (2002), Grieve (1998), Grieve et al. (1995), Masaitis (personal communication, 1999), Vishnevsky (personal communication, 1999), and Kyte et al. (1996).

and criteria for recognition of subaerial impacts discussed by Rondot (1994). The knowledge of cratering processes resulting from a bolide impact into the ocean and its effect on the environment is more tenuous. It is mostly based on modeling experiments by Nordyke (1977), Strelitz (1979), Gault and Sonett (1982), O'Keefe and Ahrens (1982), Roddy et al. (1987), Melosh (1989), van der Bergh (1989), and Sonett et al. (1991), extrapolated from submarine craters now located in a subaerial setting. The latter has consequently been exposed to weathering and erosion, which has altered their morphological features. Detailed sedimentological and process-oriented observations/discussions of known marine impacts, however, are rare. Oceanic impact, considered to be a growing field of fundamental geoscience, was recently explored by Gersonde et al. (2002) and several related contributions published in the Deep Sea Research II, v. 49 (2002).

Cometary submarine impacts were explored by Jansa (1993) after discovery of the Montagnais impact crater on the Canadian shelf (Jansa and Pe-Piper, 1987; Jansa et al., 1989) (Fig. 2); and were recently reviewed by Ormø and Lindstrøm (2000). However,

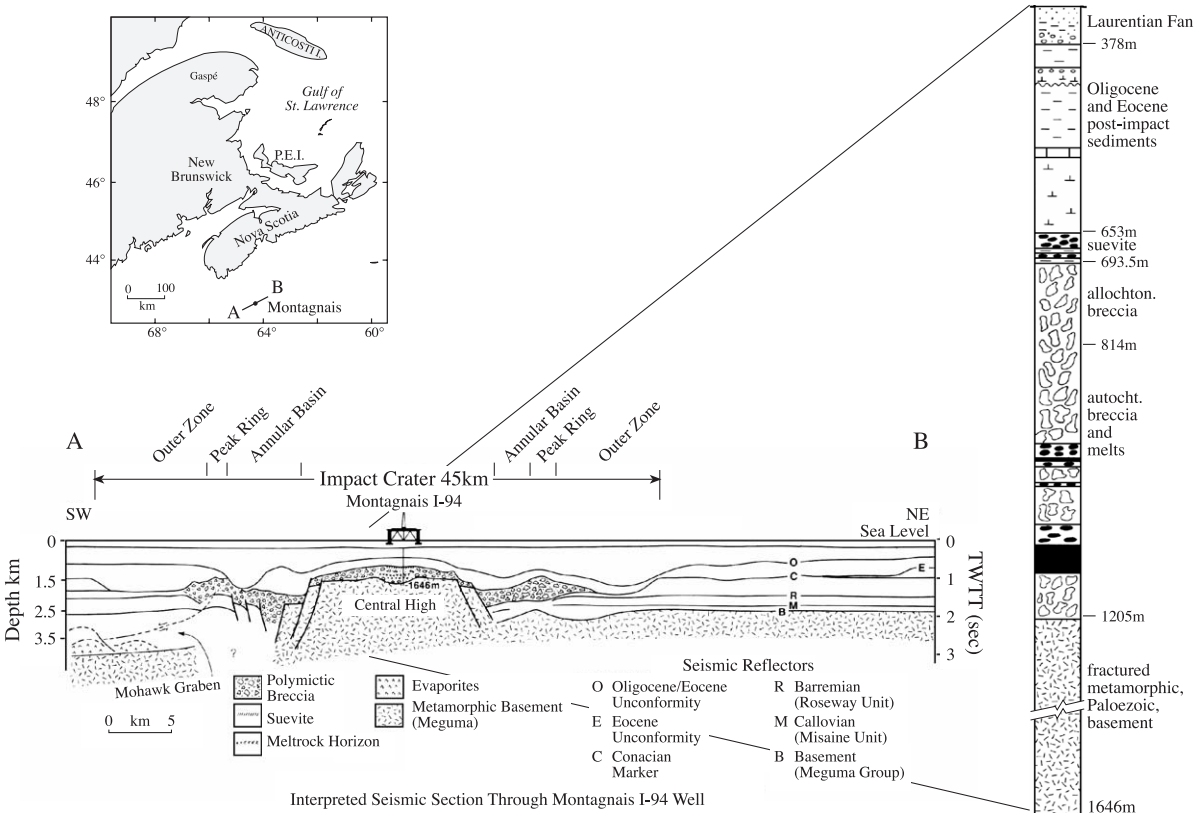

Fig. 2. The location of the Montagnais Crater, the stratigraphy of the well drilled at the center of the structure, and seismic cross-section of the Montagnais crater (modified after Jansa et al., 1989).

the latter authors concentrated mainly on the mechanical processes associated with formation of small submarine craters (<14 km in diameter) found in recent years in Baltoscandinavia. Even though they have presented valuable data for these impact craters, some of their conclusions about sedimentary processes differ significantly from ours, reached from the study of larger submarine impact craters (>40 km in diameter). We refer to craters 15–40 km in diameter as medium size and those >90–100 km as very large.

During the past 10 years, an increased number of studies have focused on sedimentary processes associated with impacts. In particular, the Chicxulub crater and the *K*/*T* boundary studies should be mentioned (e.g. Smit et al., 1992; Bohor, 1996; Sharpton et al., 1996; Stinnesbeck and Keller, 1996). Discussions of several other impact structures, such as the Lockne crater (Lindstrøm et al., 1996; Sturkell and Ormø, 1997, 1998), the Chesapeak Bay crater (Poag, 1996, 1997), and the Precambrian Hamersley Group of Australia (Simonson and Hassler, 1997; Simonson et al., 1998), include sedimentological discussion of resurge, suspension currents, and debris flow deposition. Only limited attention has been given to effects of mega-tsunamis generated by impacts (e.g. Bourgeois et al., 1988; Oberbeck et al., 1993; Smit et al., 1996; Warme and Sandberg, 1995; Warme and Kuehner, 1998; Poag et al., 1999), and almost none to the study of margin collapse associated with meteorite impacts on continental margins and shelves. With the exception of the Montagnais impact crater, none of the other large marine impacts such as the Chicxulub (Sharpton et al., 1996), Chesapeake Bay (Poag, 1997), Kara/Ust Kara (Mashchak, 1990a,b; Selivanovskaya et al., 1990), or Mjølnir (Dypvik et al., 1996; Tsikalas et al., 1998a,b,c) provide a full range of impact-related data, such as the occurrence, composition, and variability of the impact breccias, melts,

and suevite, or a full spectrum of geophysical data (reflection seismic profiles, magnetic and gravity data). But a similar range of data is available from three smaller, marine impact craters—the 380 Ma old Kaluga, which is 15 km in diameter (Masaitis, 2002), the 20 km in diameter Neugrund (Suuroja and Suuroja, in press), and the even smaller, 4 km diameter, 455 Ma Kärdla impact crater (Suuroja et al., 2001).

In this paper, we classify impact structures according to the impacting environment:

1. Subaerial impact—meteorite impacts on land, with target being various continental rocks;
2. Subaqueous/submarine impact—an impact into the marine environment, which can be either shallow submarine-neritic occurring predominantly in a neritic environment (water depth of less than several hundred meters), but also including impacts into epeiric seas, with the impact target being continental rocks and sedimentary sequences of various thickness; or deep marine-bathyal, when the impact crater was formed on the ocean floor with water several kilometers deep and the target being a thin cover of pelagic sediments underlain by ocean crust. Up to the present, no such impact crater has been identified;
3. Deep, open ocean-bathypelagic impact—when no crater was formed on the ocean bottom, but evidence for the impact is the presence of spherules and remnants of the impactor (e.g. Eltanin Impact, Kyte et al., 1981; Gersonde et al., 1997, 1999, 2002). Simonson (personal communication, 2002) suggested the need for a fourth category to which would belong impacts known only from the occurrence of ejecta; spherule layers (Simonson and Harnik, 2000), without impact locations. However, as this contribution is focused on sedimentological processes occurring in the marine environment during impacts, we do not discuss impact spherules, as they can be of both terrestrial and marine origin.

In this paper, we focus on a comparison of two of the best known submarine impact craters—the Montagnais and Mjølnir craters, which have remained buried in the marine environment, so their origin cannot be disputed. They are comparable in size and morphology (see below and Table 2) and both can be classified as complex peak ring craters. However, they differ in the composition of the target area and of the inferred impactor. This allows us to discuss more broadly sedimentary processes associated with impact cratering in a shallow sea or an ocean. We have also compiled published data from other submarine impact craters to expand the discussion of sedimentological processes associated with marine impacts and point to some differences between impacts on land and in the marine environment. We conclude with comments on an unresolved enigma: the substantial difference between the modeling of the Chicxulub impact generating mega-tsunami, and the limited geologic evidence for it.

Table 2
Apparent and transient diameters of submarine craters

Crater	Apparent diameter, D_A	Transient diameter, D_t	D_A/D_t ratio
Complex (peak ring) subaerial (terrestrial) craters			
Ries	24	20	1.2
Charlevoix	54	28	1.9
Manicougan	100	44	2.3
Sierra Madera	13	6.5	2.0
Gosses Bluff	22	11.5	1.9
Complex (peak ring) submarine craters			
Chesapeake Bay	90	35	2.6
Mjølnir	40	16	2.5
Montagnais	45	20	2.3
Neugrund	20	7	2.9

Data from Abels et al. (2002), Wilshire et al. (1972), Støffler et al. (1977), Gudlaugsson (1993), Jansa (1993), Rondot (1994), Poag (1997), and Suuroja and Suuroja (in press).

1.2. Impact crater recognition

The recognition of impact craters is usually based on a combination of geophysical, geological, petrographical, and geochemical data. The geophysical evidence comes from seismic signatures, gravity, and magnetic anomalies, whereas the geological, petrographic, and geochemical evidence includes the presence of impact breccias, stishovite and coesite, microscopic planar deformation features (PDFs) in quartz and feldspars and their partial isotropization (Jansa and Pe-Piper, 1987), changes of refractive index, phase changes (Støffler and Langenhorst, 1994; Koeberl and Reimold, 1999), presence of Ni-spinels, enrichments in iridium and siderophile ele-

ments, and the presence of various types of impact glass and spherules, etc. These criteria are applicable to both subaqueous and subaerial craters (Jansa, 1993; Gostin and Therriault, 1997), and presently, no significant differences in mineralogical, geochemical, and/or geophysical parameters have been demonstrated between these two cases. Partial isotropization of grains, which shows as cloudy extinction on single quartz and feldspar grains under the microscope (see Fig. 3A), may be more common in the submarine impacts, but a wider database is needed to confirm this distinction.

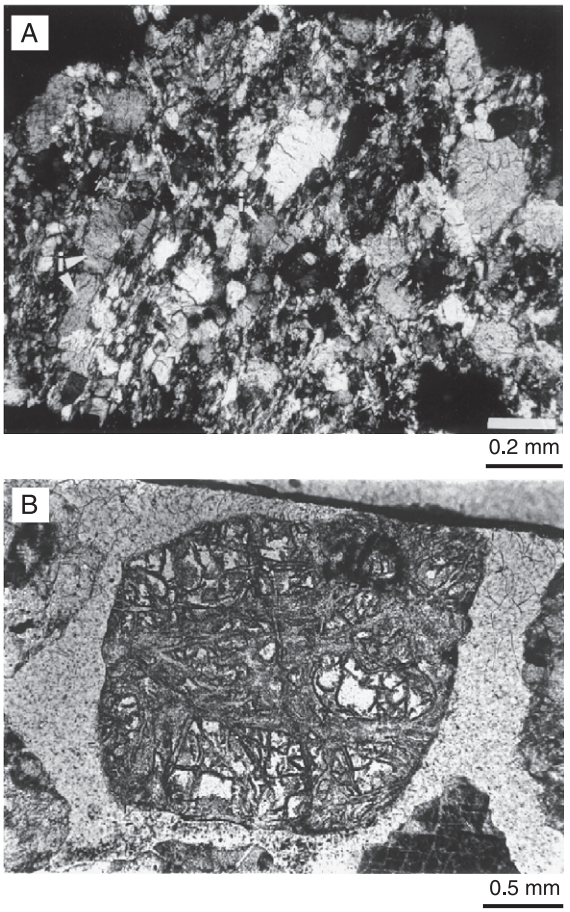

Fig. 3. (A) Isotropization of minerals in metagraywacke clast of the impact breccia, thin section (crossed polars), Montagnais I-94, 689 m. Note the extensive fracturing, undecorated shock lamellae in a quartz grain, and decrease in birefringence (shows as grayish cloud) in parts of some of the grains. (B) Highly fractured clast of metaquartzite with quartz melted into the glass along the fracture boundaries. Note the conchoidal shape of some of the fractures (Montagnais I-94, 680 m, thin section, crossed polars).

Other important impact features, such as shatter cones, have been found in both subaerial impact craters (e.g. Ries) as well as in submarine impact craters, e.g. Kara/Ust Kara (Mashchak, 1990a,b; Selivanovskaya et al., 1990).

Simonson and Harnik (2000) suggested that there could be significant and systematic differences in the composition of ejecta from subaerial (continental crust) vs. submarine (oceanic crust) impacts because the vast majority of the ejecta mass comes from the target material. Although these criteria might be applicable to Archean impacts, such differentiation is not fully applicable on Phanerozoic impacts, where all known marine impact craters were formed in shallow seas on continental crust and composition of the ejecta is similar for terrestrial and shallow marine impacts.

Characteristic lithologies, structures, and biota can assist in the differentiation between submarine and subaerial meteorite impact settings. Submarine impacts can be inferred from the presence of sedimentary features resulting from processes not occurring at subaerial impacts: e.g. formation of mega-tsunamis, high waves, strong currents, and features resulting from collapse of the central high and crater rim and the rush of returning water into excavating crater (“resurge” activity). Impacts of large bolides into marine environments will also generate tremor-like earthquakes, which could lead to fluidization of sediments, slope instability, slides, slumping, generation of turbidites, mass- and debris-flows, and avalanches. Slope instability resulting in slides, slumping, and debris avalanches can also occur during subaerial impacts, but not the development of density/suspension currents. On the other hand, subaerial weathering, erosion, and vegetation produce effects on subaerial impact sites that are not found in association with subaquatic impacts.

2. The Montagnais and Mjølnir submarine impact craters

Montagnais, located in offshore Nova Scotia, was one of the first submarine craters found (Jansa et al., 1989) still located in the ocean. Some years later, the Mjølnir Crater in the Barents Sea (Gudlaugsson, 1993; Dypvik et al., 1996) was recognized. Other

submarine impact craters were described in 1982 (Ust Kara; Masaitis and Mashchak, 1982), 1991 (Chicxulub; Hildebrand et al., 1991), 1994 (Chesapeake Bay; Poag et al., 1994), and recently the Neugrund impact crater in the Gulf of Finland (Suuroja and Suuroja, in press). Several other marine (and possibly marine) impact craters, such as Lockne, Kärdla, Granby, and Tvären, were formed during the Lower Paleozoic, impacting Paleozoic basement of the Baltic shield (Ormø and Lindstrøm, 2000). All are exposed on land. The Eltanin impact (Gersonde et al., 1997; Kyte et al., 1981) is the only documented impact into the deep ocean. Apparently, no crater formed on the ocean floor; the evidence comprises only strongly disturbed sediments and a large number of fragments from the impactor. At present, the Eltanin impact is the only known example of a bathypelagic impact where the bolide did not reach the ocean floor.

2.1. The Montagnais crater

The identification of the Montagnais impact crater (Fig. 2) (Jansa et al., 1989) was based on multichannel reflection seismic profiles, gravity and magnetic data, and detailed petrographical and geochemical studies of cuttings from an oil exploration borehole located at the center of the structure (Jansa et al., 1989). The crater is located on the outer shelf off Nova Scotia, Canada and is currently buried under 113 m of water and about 500 m of post-impact marine sediments (Fig. 2). The excavated crater is 45 km in diameter. It has a central high 1.8 km high and 11.5 km wide at the top, which is flat. A positive, circular gravity anomaly of +8 mGal is associated with the central high, whereas a negative anomaly of −5 to −10 mGal should be expected according to reigning theories (Pilkington et al., 1995). Magnetic anomalies are faint to lacking across the Montagnais structure. The Montagnais crater was formed 50.8 Ma ago (Jansa et al., 1989). The impact occurred in water 200–600 m deep by fall of a bolide 2–3 km in diameter near the shelf edge. At that time, the shelf edge was underlain by unconsolidated and moderately cemented sedimentary rocks less than 3 km thick, which in turn, overlay several kilometers of low-grade Cambro-Silurian metamorphic rocks and Devonian granites.

A 1646-m-deep well (Montagnais I-94) was drilled at the top of the central high and penetrated a 510 m thick Cenozoic succession, overlying 552 m of impact crater fill. The fill comprises two distinct types of breccia, enclosing two zones of crystalline melt rocks and one zone of a suevite, consisting predominately of glass fragments (Fig. 2). The breccia rests on uplifted and disturbed metasedimentary basement rocks of Cambro-Ordovician age, which are highly fractured, but not displaced. The basement contains shock metamorphic features, such as quartz grains with planar lamellae.

The shape of the breccia within the crater, which surrounds the morphologically higher central uplift, resembles an 8.5-km-wide donut and is generally not more than 850 m thick across the inner ring. The breccia on the central uplift is made up of two distinct types (Fig. 2). The lower part, 391 m thick, is a monomict para-autochnous breccia formed by fragmented Cambro-Ordovician metasedimentary rocks. A recrystallized melt layer, 71 m thick, is enclosed near the base of the monomictic breccia. In the upper 29 m of this lower melt layer is incorporated a large volume of partially melted and unmelted particles. The upper part of the fill is a polymictic, allochtonous breccia 161 m thick that has a 35 m thick recrystallized melt layer near its base. In addition to Cambro-Ordovician metasedimentary rock debris, the latter breccia contains fragments of both Jurassic limestones and Cenozoic sedimentary rocks. It is covered by a 40.5-m-thick layer of suevite. The structuring of the crater fill sequence is comparable to that described from the Ries crater by Støffler et al. (1977).

The maximum theoretical structural uplift of beds at the central high of impact craters should be 0.10 D_A (Grieve et al., 1981), and the width of the structural uplift approximately 0.20–0.25 D_A (Pike, 1985), where D_A = the apparent crater diameter. As the apparent diameter of the Montagnais impact crater is 45 km, these models suggest a central high with theoretical uplift of ~3 km and a width of ~9–11 km. Correlation of regional seismic reflectors across the Montagnais impact site indicates that structural uplift of the central high is about 2.5 km (Jansa et al., 1989), close in size to conventional impact crater modeling. The top of the central uplift is only slightly wider than indicated by terrestrial crater modeling.

The impact breccias which fill much of the Montagnais crater and blanket uplifted basement rocks of

the central high contain grains with shock deformation features of different intensities, diagnostic of a 35–50 GPa shock level (Jansa et al., 1989). Planar features have been observed in quartz and feldspar grains and different degrees of isotropization have been seen in numerous grains. Various degrees of melting and grain transformation into glass have also been found (Jansa, 1993) (Fig. 3). The crystallized melt of the Montagnais Crater is enriched in iridium, with concentrations up to 0.32 ppb, in contrast to the target rock, where the iridium content is much lower (0.016 ppb). No other siderophile or platinum element enrichments have been documented in the breccia and/or melts. Low Ir enrichments together with lack of enrichments in siderophile elements are considered by Bazilevskiy et al. (1984) as characteristics of comets. Therefore, the Montagnais impactor was probably an old cometary nucleus.

The rim geometry is probably one of the most easily observable differences between subaerial and submarine impacts. The Montagnais impact crater lacks an uplifted rimwall and a continuos elevated rim, which are typical morphological features of subaerial impact craters. Submarine craters such as Montagnais, Mjølnir, and Kärdla (Puura and Suuroja, 1992) probably had short lived rims during the initial phase of crater excavation. The rims and central highs were eroded and beveled by powerful currents generated at the impact time and in the aftermath by a surge of water back into the excavating cavity. As the temperature within the excavating cavity may exceed 1000 °C, the first returning water into the cavity would immediately evaporate, resulting in a strong current back flow. Ormø and Miyamoto (2002) have modeled the water back-flow following marine impacts. For the Lockne crater and the 200- and 500-m water depth models, they computed average flow velocities of 27.5 and 55 ms^{-1}, respectively. Locally, the presence of remnants of a low rim can be indicated on the seismic profiles (Tsikalas and Faleide, in press; Tsikalas et al., 1998b; Jansa et al., 1989). The rim and its weaker zones helped to channelize flow of the return water, forming resurge gullies. Currents generated by the tsunami and subsequent submarine crater collapse (Pilkington et al., 1995) may have further modified the crater rim morphology and the nature of the crater fill.

2.2. The Mjølnir crater

Knowledge of the Mjølnir crater is based on geophysical data (multichannel reflection seismic, gravity and magnetic measurements) and increasing amounts of geological information. The geophysical data are augmented by geological data of a shallow core (7430/10-U-01) drilled 30 km outside the crater (Gudlaugsson, 1993; Dypvik and Attrep, 1999; Dypvik and Ferrel, 1998; Dypvik et al., 1996; Tsikalas et al., 1998a,b,c, 1999, 2002) and by the Mjølnir core (7329/3-U-1) drilled on the flank of the central uplift (Mørk et al., 2000; Smelror et al., 2001).

The Mjølnir submarine crater, located in the Barents Sea, is 40 km in diameter (Fig. 4). It is presently covered by 350 m of water and 50–400 m of younger sedimentary strata. The crater has a central high, 8 km wide at the base, which protrudes 250 m above the crater floor (Tsikalas et al., 1998a). The estimated depth of the transient cavity is 4.5 km. The crater has only a minor upraised rim, which shows the presence of several terraces down into the crater. The terraces are bordered by faults and the outermost terrace has a rimwall about 70 m high (Gudlaugsson, 1993; Tsikalas et al., 1998b). Based on the seismic reconstructions, several depressions that cross the rimwall radially may result from post-impact gullying. The crater is filled by a 1 km thick breccia unit (Tsikalas et al., 1998a,b). It is interpreted as formed by an impact of an asteroid, or iron meteorite 1.5–2 km in diameter (Tsikalas et al., 1998b; Dypvik and Attrep, 1999) into a 200–400 m deep epicontinental paleo-Barents Sea. Based on seismic reflector correlation, the impact occurred at the beginning of the Cretaceous, during the Late Volgian–Early Berriasian (Tsikalas et al., 1998c). Micropaleontological, palynological, and macropaleontological studies from the 7430/10-U-01 core indicate an Early Berriasian age (*Berriasiella jacobi* zone) for the impact layer (Dypvik et al., 1996; Smelror et al., 2001). The target area consisted of a more or less soft sedimentary sequence of Devonian to Jurassic age, at least 6 km thick, overlying older, well-lithified sedimentary strata.

Morphologically, the crater has the shape similar to an ‘‘inverted sombrero’’, with an 8 km wide inner zone and a 12 km wide outer zone (Fig. 4). The crater is characterized by a negative gravity anomaly across the annular basin (− 1.5 mGal; − 0.03 to − 0.04 g/

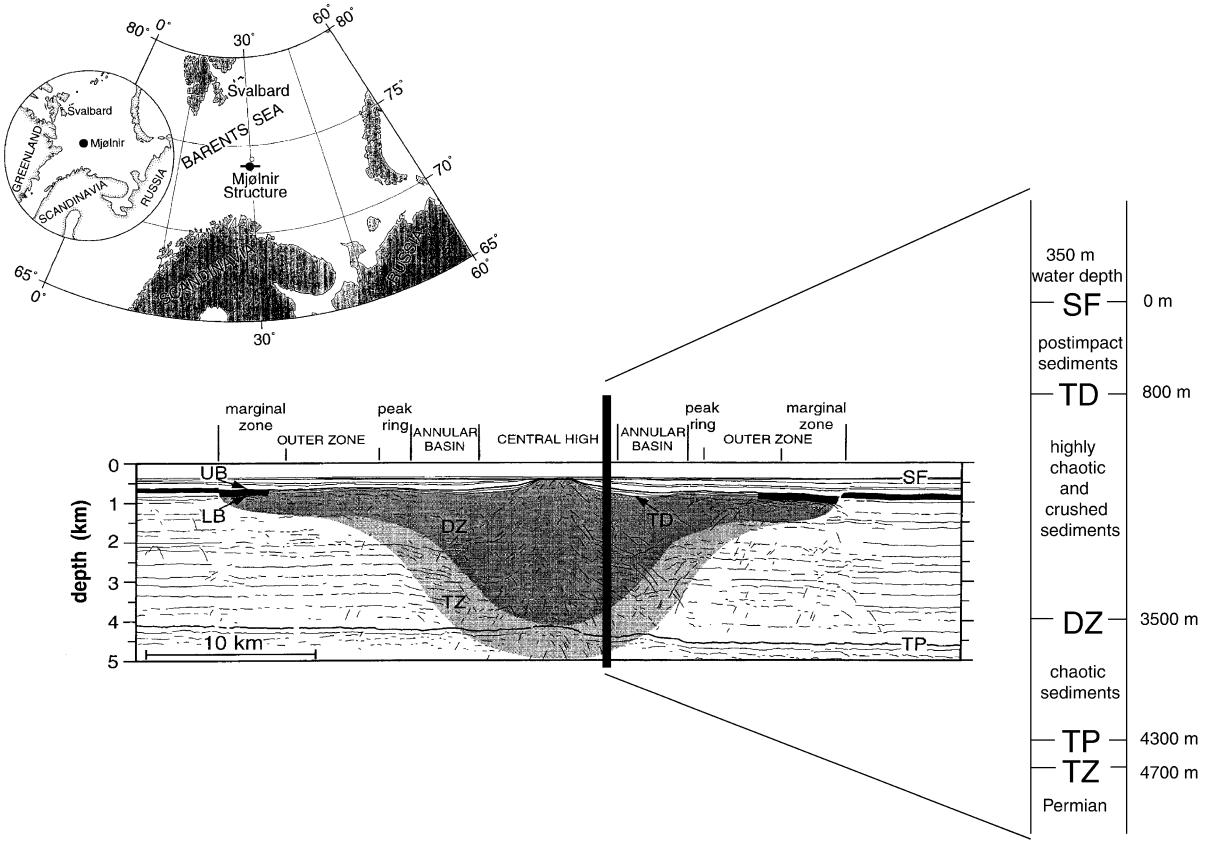

Fig. 4. The location of the Mjølnir Crater and geologic interpretation of the crater, modified after Dypvik et al. (1996) and Tsikalas et al. (1998a,b,c).

cm^3) and a weak positive anomaly across the central high (+2.5 mGal; +0.025 g/cm^3) (Tsikalas et al., 1998c). The weak gravity anomalies may reflect less brecciation in the Mjølnir Crater compared to impacts into crystalline rocks, but it might also indicate an uplift of denser underlying strata to higher crustal levels. Mjølnir is also characterized by low level magnetic anomalies. The central uplift shows no discernible magnetic anomaly and only low amplitude positive and negative anomalies are present near the transition to the annular basin. This magnetic signature can be attributed either to localized dispersed impact melts in the peripheral regions, or to dislocation of weakly magnetized platform sediments (Tsikalas et al., 1998c).

The sedimentary succession in the 7430/10-U-01 core consists of black and gray partly laminated claystones which are interrupted by a single conglomerate bed 19 cm thick (Dypvik et al., 1996). The conglomerate has an erosional base and internally consists of three upwards fining successions. Clay clasts are found along the base of the conglomerate and shock metamorphosed quartz grains are present throughout. This "basal conglomerate" (level: 47.6–47.4 m) most probably represents reworked fall-out ejecta modified by density currents, or oscillating wave surges (Dypvik and Ferrel, 1998), or by mega-tsunami waves. The main ejecta layer, which is 80 cm thick, is located at core level 47.6–46.8 m where shocked quartz and possibly also shocked feldspar, along with enrichments of elements as Ir, Cr, and Ni, have been found (Dypvik et al., 1996; Dypvik and Attrep, 1999). Dypvik and Ferrel (1998) and Dypvik and Attrep (1999) from an appearance of smectite and geochemical parameters, suggested that the total thickness of the impact

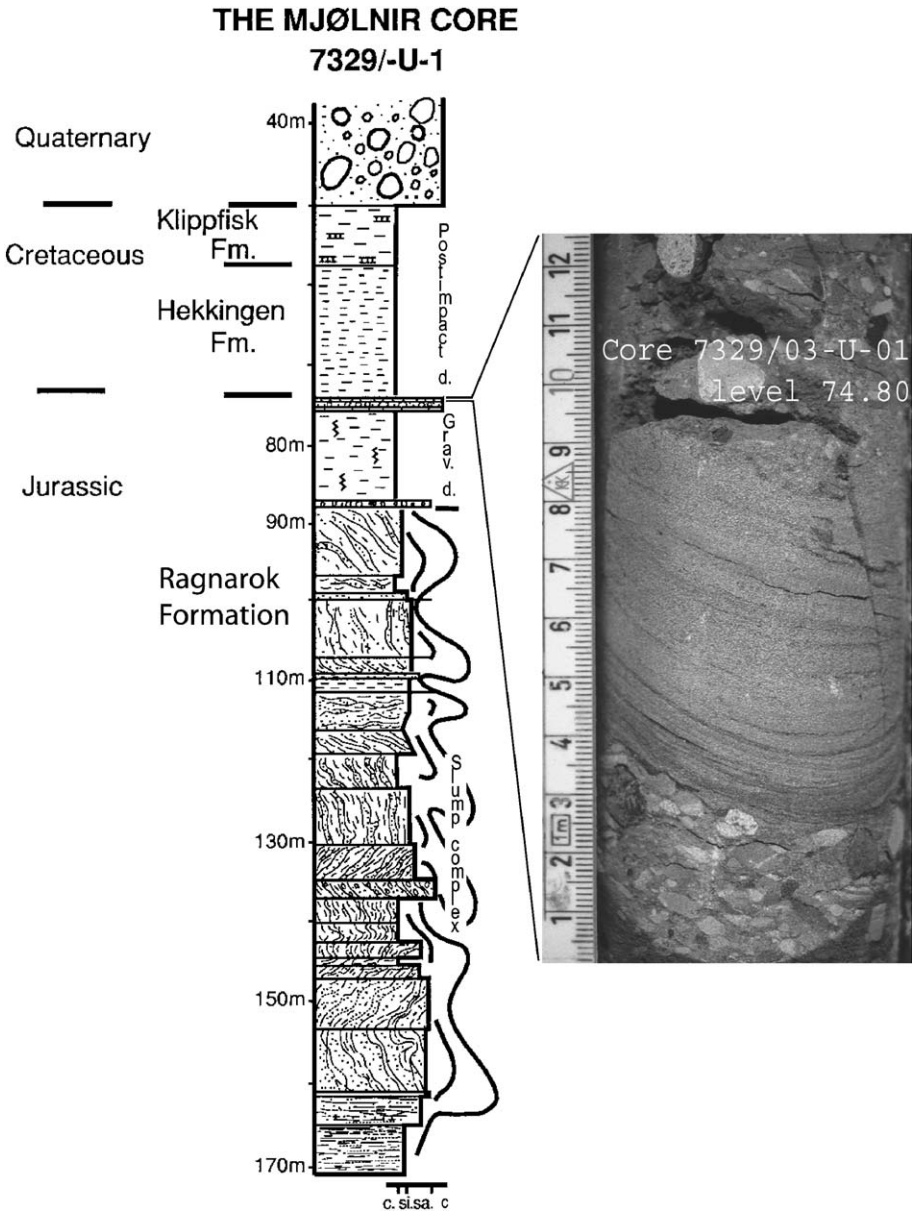

Fig. 5. The Mjølnir core log and core photograph of post-impact suspension deposits. The Klippfisk and Hekkingen Formations represent post-impact deposits, while the Ragnarok Formation consists of gravity flows and slump deposits.

related bed is 3.2 m (core-level 50–46.8 m), which is less than half as predicted by model calculations (based on Melosh, 1989). Increase in iridium in correlative beds at the Svalbard Archipelago, about 400 km northwest of the Mjølnir Crater, is considered to be evidence for impact ejecta (Dypvik et al., in preparation). Also, Zakharov et al. (1993) found an Ir peak at the Jurassic–Cretaceous boundary in the Nordvik area of Siberia which is currently located about 2500 km to the east from the Mjølnir impact site. This iridium anomaly could be result of the Mjølnir impact (Smelror et al., 2001).

The 121-m-long Mjølnir core (7329/03-U-1) (Fig. 5) was drilled near the center of the Mjølnir crater. The upper part of the core comprises of 50 m of Quaternary strata, overlying 24 m of post-impact sediments and 97 m of partly chaotic, impactite deposits. The core provides evidence only about the uppermost part of the crater fill at the flank of the central high where partly fluidized chaotic sediments alternate with thinner, more continuous units of less altered shales and sandstones (Fig. 5).

3. Comparisons of Mjølnir and Montagnais together with other known impact sites

3.1. Crater configuration and morphology

Submarine impact craters generally display configurations similar to those of larger subaerial impacts, but with several major differences as discussed below. Presently, no simple, bowl-shaped submarine crater has been found. Even a small impact crater, like Kärdla, which is 4 km in the diameter, has the character of a complex crater with a central peak (Suuroja et al., 2001). According to Melosh (1989), typical marine impact craters should have a deeper inner zone and a shallow brim forming the outer zone (see the Mjølnir cross-section in Fig. 4).

Modeling experiments (Nordyke, 1977; Strelitz, 1979; Gault and Sonett, 1982) further suggest that marine craters should be wider than terrestrial ones when formed under comparable conditions. An increase of the crater width of about 20% has been postulated by Strelitz (1979) and Melosh (1989). The width of marine impact craters should be further increased by rim erosion, due to return water-flow (resurge). This resurge may not only reduce rim height, it could almost completely obliterate the raised crater rim. Table 2 compares diameter ratios of complex marine craters and some subaerial craters. The apparent diameter (D_A) we use is the brim to brim distance including the outer zone of the crater, whereas the ''transient'' diameter (D_t) is the diameter of an annular basin including the central high area (Fig. 6). Overall, a larger (D_A/D_t) ratio seems to characterize the marine impacts, indicating a higher degree of rimwall collapse during excavation of submarine impact craters, as predicted by Strelitz (1979) and Melosh (1989). The increase in the diameter of the crater could be the result of several processes, such as wave and current erosion, the instability of unlithified and water-saturated sediments exposed at the crater walls, and subaqueous slides and slumps. In keeping with these suggestions, D_A/D_t for the Mjølnir crater is somewhat larger than that for Montagnais (Table 2). The target material in the Mjølnir area consisted of a thicker succession of soft sediments, compared to lithified limestones and basement metamorphics that were excavated to form the Montagnais crater.

Studies of planetary surfaces in the Solar System show common presence of craters with a single massive central peak, rugged and sharp at the top (Hale and Head, 1979). Both Mjølnir and Montagnais have simple, central highs which are flat on top. On seismic profiles, the central high of Montagnais resembles a guyot. This indicates that the top of the central high was located within reach of waves, where reworking and retransportation of the breccia resulted in development of a flat surface. Such reworking will also expand the size of the ''platform'' of the central high as noted at the Montagnais structure. At the Mjølnir Crater, Tsikalas et al. (1998b) suggested, from the study of reflection seismic profiles, that the flat surface of the central peak resulted from post-impact erosion. This surface is mostly a result of syn- to early post-depositional reworking by waves, like that of the Montagnais structure. Development of flat-topped central uplifts has been predicted from modeling experiments by Gault and Sonett (1982) for shallow-marine impacts. We consider this to be an additional structural feature for recognition of shallow submarine impacts.

Roddy et al. (1987) estimated that an impact of a 10-km-wide meteorite into a 5-km-deep ocean would form a higher rim uplift in the water surface than subaerial impacts. They also stated that 70% of the ejecta would come to rest within an area three times the transient crater diameter. In those calculations, however, oceanic crust of mantle composition was used as the target composition in the models, a condition satisfied only in minor parts of the present oceanic basins. The authors further concluded that differences in the strength of target materials (oceanic/mantle rocks vs. granite) were more important than the oceanic vs. land (subaerial) conditions. Their modeling experiments demonstrate that crater exca-

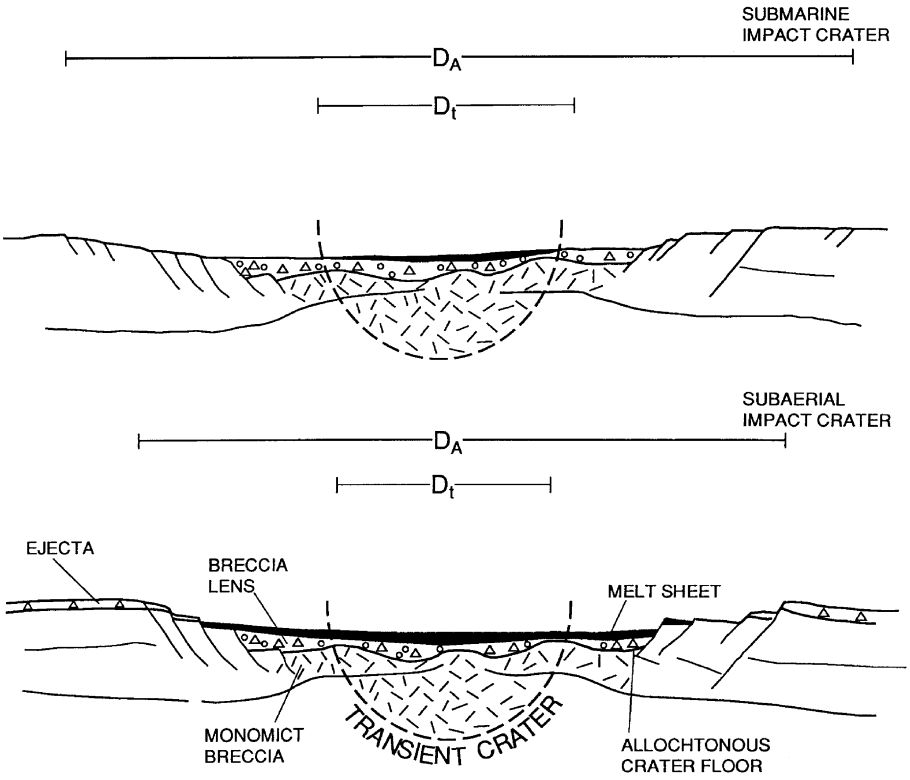

Fig. 6. Typical crater morphology for simple submarine craters (upper part) and a subaerial configuration (lower part). D_A: apparent diameter, D_t: transient diameter.

vation in both continental and marine impacts should result in the formation of sharp, uplifted rims on the transient cavity. With the rapid expansion of the transient cavity, the transient uplift of the rim decayed, but was still noticeable at the end of the modeling run, 120 s after impact (Roddy et al., 1987).

Both the Montagnais and Mjølnir craters display erosional remnants (mounds) of elevated rims (Fig. 3 in Jansa et al., 1989), but a continuous elevated rim, as seen on subaerial impact structures, is lacking (Fig. 7). Resurge channels have been identified cutting the rims of the Montagnais and Mjølnir craters (Edwards, 1989; Tsikalas and Faleide, in press). The Mjølnir crater shows a general low relief rim, possibly due to extensive post-impact crater erosion. Remnants of the rim were also noted at the Chesapeake Bay crater (Poag, 1996). We consider the lack of a continuous elevated rim to be one of most distinctive features of submarine impacts.

The rims of the Lockne, Kamensk, Gusev, Kärdla, and Kara craters are dissected by resurge gullies (Mashchak, 1990a,b; Lindstrøm et al., 1996; Sturkell, 1998; Sturkell and Ormø, 1997; von Dalwigk and Ormø, 1999). In contrast to Montagnais and Mjølnir impact craters, the Neugrund, Kärdla, and Tväreen craters display elevated rims (Puura and Suuroja, 1992; Lindstrøm et al., 1994; Plado et al., 1996; Poag, 1996; Suuroja and Suuroja, in press). All of these <10 km in diameter craters were formed in a target area where the water was very shallow, interpreted by the above authors as ranging from ~ 20 to 100 m, and the crystalline basement was covered by a very thin blanket of sediments. As strong currents and large tsunamis could not be generated due to very shallow water depths in the impact areas, the cratering processes were similar to those of subaerial impacts. This interpretation is corroborated by the presence of uplifted rims of

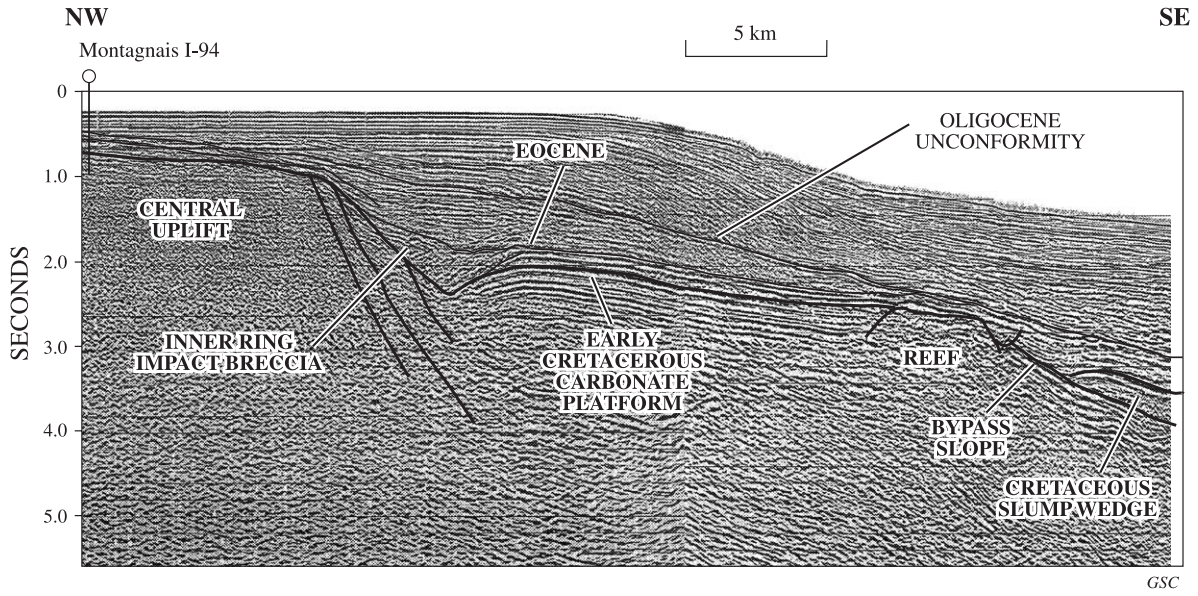

Fig. 7. Reflection seismic section oriented from the central peak of the Montagnais impact crater toward the shelf edge and deep North Atlantic ocean basin (multichannel reflection seismic line #Petro-Canada 3208-82A). Note that the outer rim is missing as well as all Late Cretaceous sedimentary sequences as result of the outer continental margin collapse. The decollement occurred at the top of Early Cretaceous carbonate platform, with the overlying Late Cretaceous sedimentary pile slumped into the deep oceanic basin.

the crystalline basement at the above-mentioned impact sites. Such morphological features indicate that processes differ between very shallow (several tens of meters) seas and neritic (several hundred meters deep) seas.

3.2. Melt rocks

The relative amounts of melted and unmelted material depend on factors such as projectile size, density, velocity, and on target properties such as density and volatile content (Melosh, 1989; O'Keefe and Ahrens, 1982) The melted material is represented by a melt pool located at the base of the transient cavity, whereas ejected melted material is found as tektites, suevite, and tagamite. When comparing submarine and subaerial impact craters, Ormø (1998) and Ormø and Lindstrøm (2000) claim the former generally have smaller amounts of melt and melt-products. This hypothesis is not supported by data from Montagnais impact crater, which contains two thick recrystallized melt pools. Tagamite and suevite are present in several of the submarine craters (Montagnais, Lockne, Avak, Tvären, Kärdla, and Neugrund).

As documented by impact craters on the Moon and corroborated by subaerial impact craters on the Earth, the impact energy associated with the formation of craters smaller than $\sim 20-25$ km in diameter is insufficient to form a melt pool. The small amounts of melts generated in such craters are normally incorporated into various solid ejecta, e.g. in the fallback suevite layer in the Ries crater (Støffler et al., 1977) and a related dispersed ejecta (moldavites).

In the Montagnais crater, two melt-zones, 35 and 71 m thick, respectively, were penetrated by the drill hole. In addition, a 40-m-thick suevite layer overlies the impact breccias on the central uplift (Jansa et al., 1989). At the Chicxulub crater, suevite is also underlain by melt rocks (Sharpton et al., 1996) of presently unknown thickness, as they were not fully penetrated by drilling. The presence of minor amounts of melt rocks is reported from the Kara crater (Mashchak, 1990a,b). Single melt particles have been described from Kärdla and Neugrund craters (Plado et al., 1996; Suuroja and Suuroja, in press). In the Lockne crater, Tørnberg (1999) suggested that the paucity of melt and suevite formation is due to explosive expansion of vapor. However, the Lockne crater is only 13.5 km in

diameter, therefore below the indicated size for formation of melt pools. In the Kara (65 km)/Ust Kara (25 km) impact-couple, Koeberl et al. (1990), Mashchak (1990a,b), and Selivanovskaya et al. (1990) suggested that high porosities in the impacted sediments resulted in fast damping of the shock wave. Consequently, higher levels of glass formation may be expected in crystalline target rock units than in impacted sediments. In the Kamensk crater (25 km in diameter), only small amounts of glass have been found, which Masaitis et al. (1991) attributed to the presence of water-saturated material, causing less diaplectic quartz to be formed by shock waves.

In the Mjølnir crater melt rocks are unknown.Tsikalas et al. (1998b) concluded from geophysical investigations that large melt-bodies are most likely lacking. The 7430/10-U-01 core from 30 km outside the crater contains smectite, a possible alteration product of impact glass (Dypvik and Ferrel, 1998; Dypvik and Attrep, 1999). As hypothesized by some of the above authors, it may appear that impacts into water-saturated targets tend to produce less melt than those in terrestrial targets; but this is not supported by the Montagnais submarine impact.

Tektites, microtektites, and spherules represent melt material jettisoned from the impact site. Melt ejecta vary in size (μm–cm) and shape, ranging from bombs to glass droplets. The latter can attain wide global distributions and in some cases can geochemically be correlated to the original impact crater (Koeberl, 1993). In some cases, the presence of tektites and/or microtektites may be the only evidence of a meteorite impact, and like Ir anomalies, may represent a useful geological marker for meteorite impact recognition. Spherules and Ir-enrichments, possibly recording impact events, have been found in the Precambrian Wittenoom Formation of the Hamersley Basin of Western Australia (Simonson, 1992; Simonson and Hassler, 1997; Simonson et al., 1998) and in South Africa (Koeberl et al., 1993). Impact spherules related to the Chicxulub impact are found around the globe. Around the Gulf of Mexico, they are commonly found along the base of fining upwards suspension deposits (Bohor, 1996; Smit et al., 1996).

The North American strewn field is a younger, smaller, but still extensive occurrence, of tektites and microtektites (Glass, 1986; Glass and Koeberl, 1999). Even though tektites are of similar age ~ 35–36 Ma, geochemical compositional differences are evident (Koeberl, 1993). There are two large known impact craters of that age, Popigai (~ 100 km) in northern Siberia (Masaitis, 1994) and Chesapeake Bay (90 km) in southeastern Virginia, USA (Poag, 1997). Both are potential sources for the two Upper Eocene ejecta layers.

Tektites or microtektites related to the Montagnais impact are unknown, as no Cenozoic rocks are preserved onshore in eastern Canada. Neither tektites nor microtektites related to the Mjølnir impact have yet been located. However, geochemical anomalies (e.g. Ir) appear in synchronous sedimentary strata in the Janusfjellet section of the Janusfjellet Subgroup at Svalbard (Dypvik et al., in preparation) and in Nordvik, Siberia (Zakharov et al., 1993).

Shaw and Wasserburg (1982) showed that tektites and impactites have geochemical compositions reflecting target compositions and tektite origins. They pointed out that sanidine spherules could be formed by oceanic impacts where both the basaltic oceanic crust and overlying sediments and seawater are involved in their formation. During the only known bathypelagic impact Eltanin, the asteroid most likely have not struck the ocean floor. The Eltanin tektites are therefore composed mostly of melted projectile material (Kyte et al., 1981; Gersonde et al., 1997; Kyte, 2002).

3.3. Mineralogical features

Glass and grains of shock metamorphic quartz (and in some cases feldspar) with typical planar deformation features (PDF) and planar features (PF) have been observed in both Mjølnir and Montagnais, as in most of the other submarine craters (Chicxulub, Chesapeake Bay, Lockne, Avak, Neugrund, Ust Kara) (Hildebrand and Boynton, 1990; Koeberl et al., 1990, 1993; Kirschner et al., 1992; Selivanovskaya et al., 1990; Lindstrøm and Strukell, 1992; Lindstrøm et al., 1996; Sharpton et al., 1996; Suuroja and Suuroja, in press). In some cases, the quartz grains also show changes in refractive index, birefringence, isotropization, and phase changes. Such structural modifications of mineral grains are present in both subaerial and submarine impacts, and grains carrying these features have been found both within and

outside of the studied craters. Jansa (1993) suggested that the common occurrence of decreased birefringence in quartz and partial melting of grains could be one of the characteristic features of subaqueous impacts, but not enough data are yet available to confirm or refute this hypothesis.

3.4. Geochemical changes

Meteorites, asteroids, and comets can leave their geochemical signature in the impacted sediments. In both the Mjølnir and the Montagnais craters, Ir anomalies are present. The melt rock in the Montagnais Crater shows only a minor increase in Ir concentration (0.1–0.3 ppb), above a depleted background value of 0.016 ppb (Jansa et al., 1989). For the Mjølnir Crater, ejecta 30 km outside the crater rim display an Ir peak of 1 ppb (Dypvik and Attrep, 1999; Dypvik et al., 1996). Based on the mutual presence of siderophile elements at the latter site and the large differences in Ir concentrations between the Mjølnir and Montagnais craters, differences in the two impactors should be expected; a comet in the Montagnais and an asteroid or (?iron meteorite?) in the Mjølnir case (Jansa, 1993; Dypvik and Attrep, 1999). Much closer identification of the impactor composition was obtained by geochemical and petrographic analyses of the Eltanin meteorite fragments (Kyte, 2002). These indicate that the bolide was most likely composed of a fine-grained polymictic breccia, with debris similar in composition to howardites and mesosiderites.

In a Na-rich marine environment, impact glass should alter to smectitic clays. This has been documented by alteration of Chicxulub impact glass in the Gulf of Mexico (Sigurdsson et al., 1991) and suggested for smectite enrichment associated with the Mjølnir impact (Dypvik and Ferrel, 1998). Based on lower Na activities and higher K activities in terrestrial compared to marine environments, terrestrial glass alteration would most probably proceed to more illitic clay minerals. Impact-melts are almost instantly buried under collapsing material from crater walls and central high and by fall-back and wash-back breccias. Therefore, the impact glass exposure to marine water will be minimal and early diagenetic changes slowed, as indicated by the Montagnais impact site, where still some fresh glass is present (Jansa and Pe-Piper, 1987). Pore water circulation and increasing burial with increase in pressure and temperature could cause late diagenetic alteration of the original glass into clay minerals and zeolites.

More generally, Gerasimov et al. (1999) pointed out that water could play a significant role in the processing of silicate material during marine impacts. Together with the shock-induced decomposition of water-bearing silicates and physical vaporization of ocean water, several chemical effects are involved, such as destruction of water molecules, formation of hydrous silicate structures, and synthesis of new phases by chemical reactions involving hydrogen and oxygen. For biological extinctions, it is important that increase in oxygen in the presence of sulphur and water vapor can result in direct formation of H_2SO_4 in the vapor cloud. Gerasimov (1999) and Gerasimov et al. (1999) further indicated that increasing the water content of sediments in the target area may increase the geochemical reduction of carbon, and thereby contribute to increased production of elementary carbon and synthesis of complex hydrocarbons. This might be the explanation for the high amounts of elementary carbon present, e.g. in the Gardnos impactite (French et al., 1997).

3.5. Impact breccias

The breccias filling impact craters result from combinations of various processes active during and after crater excavation, including the ballistic ejection of excavated material and its reworking back into the crater by slides, slumps, waves, and currents. Five breccia types associated with marine impact craters have been recognized from detailed sedimentological studies: (a) breccia formed during the excavation stage in a transient crater (monomictic, autochthonous), (b) fall-out breccia (polymictic, allochtonous), (c) fall-back breccia (polymictic, para-autochthonous), (d) slump-back breccia from crater walls and central highs (polymictic, para-autochthonous), and (e) retransported breccia from outside of the crater (polymictic allochtonous). More detailed impactite classifications have been presented by French (1998) and Masaitis (1999). In the Montagnais impact structure, the monomictic, autochthonous breccia at the bottom of the structure is overlain by a polymictic, allochtonous breccia, which most probably represents a mixture of fall-back and

retransported material. It is overlain by a fall-back polymictic para-autochthonous breccia represented by the suevite. In the surroundings of the Mjølnir crater, reworked fall-out ejecta have been identified in a core located 30 km beyond the crater. The reworked ejecta (19 cm in thickness) occur as three fining-upwards beds representing deposition from turbidity currents (Dypvik et al., 1996). Breccias were also drilled at the flank of the central high (Fig. 5) (the Mjølnir core).

The Mjølnir core (totaling 121 m), drilled along the flanks of the central high, shows more than 30 m of post-impact sediments overlying 83 m of chaotic, slumped, and folded Mesozoic sediments deposited on the crater floor. The latter consists of slumped and fractured Upper Triassic to Lower Jurassic sediments uplifted along with the central high. The succeeding 14 m was deposited by debris flows, mud flows, and turbidity flows, triggered and moved along the slopes of the central high. Twenty-four meters of Lower Cretaceous post-impact sediments covers the crater-related sediments, thereafter the Quaternary strata.

Based on detailed geophysical analyses, Tsikalas et al. (1998b) indicated that the Mjølnir structure may have been filled by two different breccia units: an upper allochtonous breccia, 1.1–1.3 km thick, consisting of fallback and wash-back/resurge material; and a lower autochthonous breccia up to about 2–3 km thick.

Theoretically, the maximum thickness of a breccia lens filling an impact crater is roughly half of the rim to floor depth of the crater itself (Melosh, 1989). Comparisons suggest that the crater-filling breccias within subaerial craters are thinner than those in marine impact craters. In the Montagnais crater, the breccia overlying the central uplift is 552 m thick, whereas it is more than 850 m of thickness at the inner ring. The breccia on the central high is intercalated with several layers of recrystallized melt and has an overall thickness which is greater than in subaerial impact craters of comparable size (Jansa, 1993; Jansa et al., 1989; Grieve, personal communication). This difference arises because resurge currents transport excavated material back into the cavity from outside the crater. This process does not occur during terrestrial impacts. This provides another criterion for distinguishing terrestrial from marine impact craters.

4. The sedimentology of bolide impacts

Catastrophic event deposits, including those generated by a tsunami, caused by an asteroid impact into a marine environment were the subject of a Special Issue of Sedimentary Geology (Vol. 104, 1996). More recently, Shiki et al. (2000) discussed some of the recognition criteria for tsunami deposits. However, descriptions of sedimentological features generated by impact-triggered tsunamis are rare. Hartley et al. (2001) have described a convincing Pliocene example from Chile, which Felton and Crook (2003) suggest may have been generated by the Eltanin impact event in the SE Pacific.

4.1. Sedimentation within the crater

Avalanches, slides, and slumps are generated from the central highs and the walls of an expanding crater during excavation of the impact cavity. The majority of the ejecta in subaerial impacts is transported solely by air, whereas in marine impact craters, air-borne ejecta are often reworked by currents along the sea bed, or within the excavating cavity. The presence of autochthonous breccia dispersed within melt horizons at the Montagnais crater indicates that debris was transported down to the cavity floor by avalanches and debris flows from the walls of the excavating crater before hitting the final rise of the central high. The overlying para-autochthonous, polymict breccia and suevite provide evidence for incorporation into the cavity of ballistically ejected particles and fall-back breccia during later periods of cavity excavation. In the Mjølnir Crater, about 14 m of chaotic sediments, most probably resulting from submarine slumps, debris flows, and/or suspension currents, occurs in the upper part of the crater fill succession (Mørk et al., 2000). These were derived and transported from the central high into the surrounding crater. Tsikalas et al. (2002) developed a quantitative model for porosity changes resulting from the Mjølnir impact. From density and travel time distribution, they concluded that the porosity in the crater increase by 6.3% immediately after the impact, but was reduced by 2.5% after the crater was buried.

In the Lockne crater, slump deposits and turbidites are present within the 200 m thick sedimentary succession filling the crater, where reworked ejecta

are mixed with impactites, fractured and melted target rocks and fragments of marine background sediments (Lindstrøm et al., 1996; Ormø and Miyamoto, 2002). In other marine impact craters, e.g. the Avak (Kirschner et al., 1992), Chesapeake Bay (Poag, 1997; Poag et al., 1994), Chicxulub (Sharpton et al., 1996), Kärdla (Puura and Suuroja, 1992), and Neugrund (Suuroja and Suuroja, in press), turbidites and sediments deposited by slumps, debris flows, and suspension flows have also been identified. At the Chicxulub Crater, an impact breccia up to 500 m thick was penetrated in several wells drilled in the outer ring, 150 km from the center of the crater (Sharpton et al., 1996; Ward et al., 1995). This breccia is poorly sorted and composed of sand to gravel sized, angular to subrounded fragments of dolostone, anhydrite, limestone, melt rocks, and altered glass. It was interpreted by Ward et al. (1995) as a debris flow deposit. In the Chesapeake Bay Crater, the Exmore Breccia is about 250 m thick (Poag, 1996), comparable in thickness to the sedimentary formations interpreted as resurge sediments in the Lockne Crater (Lindstrøm et al., 1996; Ormø and Lindstrøm, 1999).

4.2. Sedimentation outside the crater

Shock-generated sea waves, gigantic tsunamis, and resurge currents all result in transport and reworking of marine surface sediments together with ballistically transported ejecta. Consequently, suspension, turbidity currents, grain flows, mud flows, debris flows, and resuspension of finer particles deposits can occur depending on the geographic location of the impact site: i.e. on the shelf, nearshore, or proximal to the shelf edge, in a shallow sea, or in the deep bathyal ocean. Ivanov (1999) indicated that a cometary impact may generate currents that can reach velocities up to 100 m/s at a distance of 20 km from the impact site. A 19 cm thick composite turbidite related to the Mjølnir impact has been identified in core 7430/10-U-01. Similar sedimentary facies from the Chicxulub crater excavation have been found at Arroyo el Mimbral (Mexico), Beloc (Haiti), and several other localities around the Gulf of Mexico (Smit et al., 1996), where a siliciclastic unit is composed of a mixture of replaced impact spherules and sand. This unit, previously interpreted as a tsunami-like impact-wave deposit (Smit et al., 1992), was reinterpreted by Bohor (1996) as a succession of gravity deposits channelized through incised canyons. Turbidity currents and gravity flows generated by the Chicxulub impact in northeastern Mexico were also described by Adette et al. (1996) and recently discussed by Bahlburg and Claeys (1999). Yancey (1997), in a study of Cretaceous–Tertiary boundary at Brazos River, Texas, documented structures at the top of the *K*/*T* boundary layer indicating deposition under conditions of waning wave activity. At the Montagnais impact site, such deposits have not been identified, since only drill bit cuttings have been recovered from the Montagnais drill site as well as from the other nearest oil-exploratory drill site located 50 km to the southeast of the Montagnais.

Turbidites, debris flows, or any other marine gravity deposits triggered by seismic events, tsunamis, slope failures, or by a meteorite impact are sedimentologically similar, despite having different trigger mechanisms. The only distinguishing criteria are the presence of either impact-produced sedimentary particles, such as various forms of melts, impact spherules, and minerals such as quartz with planar deformation features and a distinctive geochemical composition, such as an iridium anomaly.

Along the crater margin and outside the crater rim, resurge sediments may be present. At the Montagnais impact site, deep incisions and channels cutting the rim have been interpreted from the seismic data by Edwards (1989) and Jansa et al. (1989). These channels can be followed up to 22 km northwest from the crater rim, with their depths decreasing in that direction. They are resurge gullies; however, as they demonstrate several periods of erosion, it is uncertain how much their shapes were modified by later, post-impact bottom current activity. Ormø and Lindstrøm (1999) note that resurge gullies should be common in marine impacts as they can be recognized in the Lockne Crater and the Kamensk structure. Across the rim of the Mjølnir crater, depressions seen on the reflection seismic profiles may represent resurge gullies modified by later compaction (Tsikalas and Faleide, in press).

Impact-generated suspension currents, mass flows, and tsunamis can alter the sea bed as well as the morphology of neighbouring coastal areas. The effects would, however, vary according to impact location, regional geology and topography, water depth and

impactor size, its composition, and velocity. Even if the bolide itself does not reach the sea bed (e.g. the Eltanin impact, Gersonde et al., 1997), impact-generated waves could severely disturb the sea floor in shallow-water areas. The most severe disturbances should be expected on shelves, as impacts that can disturb deep ocean floor may be rare.

Modeling of the interaction of a typical stony asteroid (density of 3.32 g/cm^3 and velocity of 20 km/s) with the atmosphere indicates that a bolide of 300 m to 1 km in diameter will impact the Earth surface every 1000–300,000 years (Shoemaker et al., 1990; Toon et al., 1994; Crawford and Mader, 1998). Bolides larger than 1 km in diameter will excavate sea floor in 5000 m deep ocean (Crawford and Mader, 1998; Ward and Asphaug, 2002). The latter authors calculated that a 1.1-km diameter asteroid travelling at 17.8 km/s would blow a cavity 19 km in diameter at the sea floor at a 5-km-deep ocean. Therefore, there is a high probability for at least three large impacts within any 1 million year time window, some of which inadvertently would be in deep ocean. Since impacts of such bolides are known to occur in the shelf areas and shallow seas, the lack of impact structures in the abyssal ocean is most probably due to the young age of the ocean floor and our lack of detailed knowledge of its morphology, rather than lack of impact structures.

4.3. Impact-induced tsunami deposits

A gigantic tsunami can result from the impact of a bolide into the ocean. Ahrens and O'Keefe (1983) calculated that the tsunami will contain kinetic and gravitational energy amounting to some 7–9% of the impact energy. An event of the size of the *K*/*T* impact is expected to generate tsunami effects about 10^3 times more intense than those of the largest historic earthquakes. Modeling experiments have conclusively demonstrated that at least two, or even three, "tsunami-like" waves would be generated by an impact into an ocean (Gault and Sonett, 1982). Additional tsunami-like waves could be triggered by slumps and slides along the crater highs and margins. The depositional outcome will be a stratigraphic unit with a complex lithological composition and structure. It may include multiple erosional surfaces and most likely be comprised of several beds. According to the calculations of Ahrens and O'Keefe (1983), a mega-tsunami, generated by "*K*/*T* type" bolide impact, would decay to a height of 150 m half-way around the world and would attain a maximum speed of about 0.2 km/s. According to those estimates, the mega-tsunami would inundate the low lying coastal areas on the Earth within 27 h. Therefore, any gigantic tsunami deposit generated by a bolide impact will be deposited within a very short time interval of minutes to hours, rarely of days. van der Bergh (1989) suggested that an impact forming a 150 km in diameter wide crater in 5 km of water-depth would create a 1300-m-high tsunami within a 300-km radius decreasing to a 100-m-high tsunami within a 10,000-km radius of the impact. It should be noted that the possibility for information of such waves is highly discussed.

According to Jansa (1993), the Montagnais impact created a 200-m-high wave 300 km from the crater, whereas Tsikalas et al. (1998b) suggested that the Mjølnir impact formed a 30–60 m high wave at a distance of 50 km from the impact site. If the Mjølnir dimensions are applied to the equations of van der Bergh (1989), however, similar values as those found for the Montagnais cratering are achieved (Dypvik and Attrep, 1999). The search for direct tsunami-related sedimentation caused by the Mjølnir and Montagnais impacts has so far proven unsuccessful, even though such gigantic tsunami waves should result in a maximum horizontal orbital velocity of 21 m/s of water near the sea floor at the shelf, and a velocity of $\sim$ 57 cm/s at distance of 1000 km in 5000 m deep ocean (see below). Therefore, based on cited calculation these impacts should produce recognizable erosion on sea floor and disconformities at the shelf area. The effects may be subdued due to poorly consolidated, water-saturated sediments on the sea floor.

The gigantic tsunamis formed by the five times larger Chicxulub impact must have generated suspension currents, turbidites, mass flows, and debris flows in combination with slumping and sliding across the 200-km-wide Gulf of Mexico and in the surrounding depositional areas (Bohor, 1996; Ocampo et al., 1996; Smit et al., 1992, 1996). The *K*/*T* boundary deposits in Mexico and around the Gulf of Mexico are characterized by the presence of coarse-grained, basal beds rich in spherules and mud flakes. The basal unit grades into fining upward sandstone sequences, which are commonly capped by rippled sandstones and siltstones carrying both Ir enrichments and Ni-rich

spinels (Adette et al., 1996; Bohor, 1996; Rocchia et al., 1996; Smit et al., 1996; Stinnesbeck and Keller, 1996). Impact-related deposits at the *K*/*T* boundary consisting of a mixture of chalk clasts and normally graded sandstones were identified in Deep Sea Drilling Sites in the Gulf of Mexico, Caribbean, and Blake Nose (Alvarez et al., 1992; Smit et al., 1996; Bralower et al., 1998; Moore et al., 1998). The sandstone beds, which have a complex architecture, accumulated at neritic to upper bathyal depth. Smit et al. (1996) and Smit (1999a,b) came to the conclusion that although these beds locally differ, they appear to form a consistent depositional sequence within the *K*/*T* sandstone complexes. The characteristics of the deposits at a distance <800 km from the Chicxulub impact structure are a sharp erosional base and poorly sorted coarse-grained pebbly sandstone containing recrystallized spherules with vesicles (interpreted as impact ejecta). The overlying, upward fining fine-grained sandstones and siltstones contain increased concentrations of iridium. According to the above authors, redeposition by a series of large tsunami waves is the most likely explanation for the organisation of the *K*/*T* sandstones.

Impact-generated gigantic tsunamis may erode the sea-bottom in shelf regions and result in the formation of mud-clast conglomerates or breccias in shelf environments, as documented by Bourgeois et al. (1988) at the Cretaceous–Tertiary boundary near the Brazos River, Texas. Such beds may contain older rocks and ejecta in addition to reworked contemporary sediments. Giant tsunami shelf deposits could contain pelagic and deep benthic microfauna intermixed with neritic forms and exotic material transported by backflow from coastal erosion. Such a possible tsunami-generated deposit at the Cretaceous–Tertiary boundary was identified in Pernambuco, northeastern Brazil (Albertao and Martins, 1996). It is a graded bioclastic/intraclastic packstone with an erosive base, which contains microtectites and shock-metamorphosed quartz grains. It is overlain by a 2 cm thick marly bed with increased iridium concentrations of 0.69 ppb.

A possible impact-generated tsunami breccia was described from the Upper Devonian in southern Nevada by Warme and Sandberg (1995). It is the Alamo Breccia, over 50 m thick, with megaclasts 500 m long and 90 m high at the base and covers an area of 10,000 km^2. The breccia consists of up to five graded units of shallow water carbonate with gravel-size clasts near the base and mud-size particles at the top. Warme and Kuehner (1998) reinterpreted the Alamo Breccia as encompassing a within- or near-crater breccia, with the thinner outer sequence resulting from the uprush of tsunamis that transported breccia material from deeper water. The presence of shocked quartz and spherules supports a bolide impact origin.

4.4. The mega-tsunami dilemma

From both modeling experiments and theoretical calculations, the effects of mega-tsunamis generated by a "*K*/*T*-type bolide" should be recognizable at oceanic depths half-way around the world (Ahrens and O'Keefe, 1983; van der Bergh, 1989). The wavelength of a typical tsunami exceeds 200 km; therefore, it represents a so-called "shallow-water wave", the speed of which is determined by water depth. Such waves move at high speed across the open ocean, well over 700 km/h. A velocity of 720 km/h has been suggested for the *K*/*T* impact-generated mega-tsunami wave by Ahrens and O'Keefe (1983). From marine impact modeling, the latter authors and van der Bergh (1989) suggested that mega-tsunami waves generated by "*K*/*T* size" bolides will have heights of 100–150 m half-way around the world. The maximum horizontal orbital velocity (u_m) near the sea-floor for the water movement associated with a "shallow wave" assuming a 200 km wave-length at the depth of 5000 m can be calculated by the equation given by Pickering et al. (1991):

$$u_m = \frac{Hc}{2h}$$

where $c=(gh)^{0.5}$ = shallow water wave speed; g = gravitational acceleration; h = water depth; H = wave height.

For a tsunami height of 100 m, the near bottom velocity at the depth of 5000 m would be 2.21 m/s, which is much higher than the critical velocity needed for erosion of carbonate ooze (15–35 cm/s), or unconsolidated clay and silt grains (10–20 cm/s; Postma, 1967). Far more destructive conditions will occur as such a wave approaches a shelf edge. Assuming the same wave height as above and water

depth at the shelf edge of 200 m, the velocity of the approaching wave near the sea bottom will increase to 11 m/s, with the ability not only to erode but also to move boulders and blocks. As mega-tsunami waves approach the coast, the abrupt shoaling of water depth will cause further dramatic increase in wave amplitude, as the uniformly distributed wave energy is compressed and released (Pickering et al., 1991). Secondary water movement, such as that generated by back flow from shallow-water and coastal run-up, together with offshore-directed surges and associated sediment gravity flows (e.g. turbidity currents), will be capable of generating a wide range of bed forms.

Mega-tsunamis can thus leave a varied depositional imprint of their passage. This is characterized by chaotic mixing of sediments from different coastal environments and of diverse grain sizes. Intuitively, it seems likely that back flow surges would be of sufficient magnitude to move all normally available grain sizes. Goff et al. (2001), who summarized diagnostic characteristic of tsunamis, noted that blocks up to 750 m^3 can be moved as well as sand and mud. Even larger objects could have been moved by *K*/*T* mega-tsunami.

So, why has so little evidence for the *K*/*T* mega-tsunami been found around the North Atlantic and none in the deep ocean basins, except for the Gulf of Mexico? The only undisputable evidences for a distal tsunami deposit generated at the *K*/*T* boundary are the coarse grained sedimentary beds sandwiched within the shaly strata deposited on the shelf at Braggs and Brazos River, Texas (Bourgeois et al., 1988) and in northeastern Brazil (Albertao and Martins, 1996). We can suggest several reasons for the lack of evidence of the *K*/*T* mega-tsunami outside of the Gulf of Mexico. Strelitz (1979) has indicated that the complexities may arise from manifested nonlinearity of the waves and conversion of the coherent energy into turbulence, which tends to greatly reduce catastrophic run-up. Another probably more important factor is the physiography of the impact target region. The theoretical calculations for impact-generated tsunami were made for the deep open ocean, but the Chicxulub impact occurred on a shallow carbonate shelf, rimmed by a reef barrier at the shelf edge, and adjacent to the deep basin of the Gulf of Mexico. The latter basin was at that time partially restricted by a shallow water carbonate platform barrier to the northeast, by the Cuba/Hispanola volcanic arc to the south, and by land to the west (Fig. 8). These morphological constraints would result in wave refraction and interference leading to a decrease in wave energy outside of this region.

Some confirmation of this hypothesis is provided by the Deep Sea Drilling Program around the Bahamas. There, Austin et al. (1988) reported the commonly occurring unconformities associated with coarse-grained and pebbly beds separating Early Tertiary and Late Cretaceous units. They interpreted these as talus or sediment gravity deposits derived from the Bahama Bank. However, they did not consider that such major and widespread erosion and sediment reworking might be the result of a Chicxulub mega-tsunami, as we intuitively suggest.

A third reason for the difference between observations and the modeled mega-tsunami is the large differences in published model results. How good is our knowledge, for example, Crawford and Mader (1998) note that in the literature, a 1-km asteroid travelling at 20 km/s has been estimated to generate a 200-m-high tsunami after a 1000 km run out. But Crawford and Mader (1998), using the same parameters, modeled the tsunami wave amplitude using the same parameters as only 6 m.

An impact-generated mega-tsunami on a shelf might be better modeled by examining the effects of submarine volcanic eruptions. Historic records of such eruptions (Krakatoa, Santorini) show that the damage was limited to sites near the eruptive source (Cita et al., 1996).

4.5. Continental margin edge failures

Based on studies of the Montagnais impact crater, Jansa (1993) suggested that continental margin-edge failures, collapse, and related faunal mixing could be caused by large bolide impacts onto the shelf. Morphologically, the shelf edge seaward from the Montagnais Crater shows a large semi-circular reentrant where the slope is gentler than in the surrounding area, accompanied by a sedimentary bulge at the toe of the continental slope (Bathymetric map 801-A, Canadian Hydrographic Service, Ottawa, 1990). Both features suggest collapse of the shelf edge triggered by the impact-generated shock waves. Once disturbed, the material could have moved downslope, being redeposited by slides, slumps, avalanches, and debris

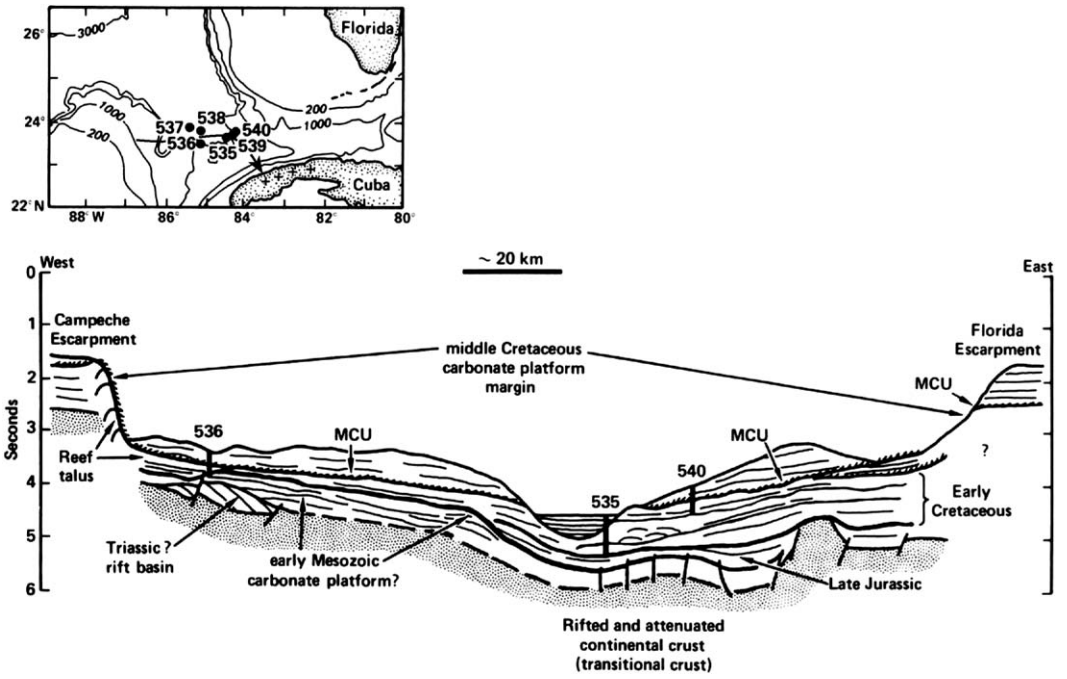

Fig. 8. Insert shows the location of Deep Sea Drilling Sites in the Gulf of Mexico and generalized location of *K*/*T* megabreccia in Cuba. The schematic section across the Gulf of Mexico from the Campeche to Florida Escarpment is based on a reflection seismic line interpreted by Schlager et al. (1984). The trough on flank of which Site 535 is located was interpreted by Schlager et al. (1984, Fig. 4) as a half graben or graben. In contrast, we interpret the "trough" as a locality were the *K*/*T* megabreccia was channelized by erosion of the trough (note that most of the Upper Cretaceous pelagic sedimentary strata underlying the trough are missing. MCU = Mid-Cretaceous Unconformity of Schlager et al. (1984), here reinterpreted as *K*/*T* boundary unconformity).

flows. This hypothesis remains untested as the deep basin off the Montagnais structure has not been drilled, but some support is provided by reflection seismic data collected in the crater vicinity. The seismic line (Fig. 7) shows that the crater rim is missing at the shelf-edge, together with all Upper Cretaceous strata down to the top of the Lower Cretaceous carbonate platform. The seaward-dipping surface at the top of the carbonate platform most probably represents the decollement surface.

Better documented is the continental shelf edge failure triggered by impact-induced seismic activity in the Gulf of Mexico and Caribbean (Pszczolkowski, 1986; Alvarez et al., 1992; Bralower et al., 1998; Grajales-Nishimyra et al., 2000; Takayama et al., 2000). Remobilized sediments of approximately *K*/*T* boundary age were recovered in the Gulf of Mexico during DSDP Legs 10 and 77. Pszczolkowski (1986) suggested that *K*/*T* deposits at sites 97 and 540 might bear on the impact hypothesis. Bralower et al. (1998) noted that the *K*/*T* boundary in the Gulf of Mexico and Caribbean is normally marked by a bed a few tens of centimeters thick with mixture of lithologies, which they named "the Cretaceous–Tertiary boundary cocktail". They suggested that this was deposited by a gravity flow, apparently triggered by the collapse of continental margins around the Gulf of Mexico. Alvarez et al. (1992) restudied cores from sites 536 and 540, which are 93 km apart (Fig. 8) and located in the deep-water entrance to the Gulf of Mexico, between Yucatan and Florida. The 45-m-thick sequence of coarse-grained deposits at Sites 536 and 540, according to Alvarez et al. (1992), consists of poorly sorted pebbly mudstone containing chalk, mudstone, and bioclastic limestone clasts (unit 2). It is overlain by cross-bedded sandstone with angular clasts of chalk and bioclastic limestone (unit 3) that grades up into chalk (unit 4). Units 3 and 4 contain spherules, shocked quartz, and glass fragments, and increased iridium concentrations.

Alvarez et al. (1992) interpreted the cross-bedded sandstone (unit 3) as the result of reworking of the ejecta on the deep sea-floor by the tsunami. Both Alvarez et al. (1992) and Bralower et al. (1998) accepted the interpretation of Schlager et al. (1984) that the Albian to Cenomanian 100-m-thick limestone sequence at Site 536 (Unit 1) represents an autochthonous substratum. Unit 1 is lithologically distinctly different from the underlying strata, composed of pre-Aptian brown dolomite.

We have restudied data from the above DSDP Legs which, in combination with the result of field studies of the Cretaceous strata in Cuba by one of the authors (Jansa), lead us to further modify the interpretations of Buffler et al. (1984), Schlager et al. (1984), Alvarez et al. (1992), and Bralower et al. (1998). At site 536, only 4% of one core was recovered from the Lower Cretaceous limestone sequence (Unit 1). It was interpreted by Schlager et al. (1984) as a drilling breccia, composed of clasts of shallow water limestones, well-sorted grainstones, radiolarian mudstone, and nannofossil chalk. The coarse material in the limestones consists of gravel-size fragments of rudists and debris of corals, gastropods, dasycladacean and codiacean algae, and a few benthic foraminifera. This shallow water fauna led Buffler et al. (1984) to interpret the sequence as carbonate platform talus, shed downslope into deep-water environments, which was the most logical explanation at that time.

A mega-breccia, in part similar in texture and composition to the breccia in Site 536, outcrops in Sierra del Rosario, Cuba. It is up to 400 m thick and can be followed for almost 800 km from western Cuba to near Penalvar, east of Havana. The thickness and grain-size decrease eastwards. The lower part of the mega-breccia at Sierra Rosario is massive, boulder to pebble size, unsorted, and clast supported with clasts containing frequent rudists, corals, orbitoid foraminifera, benthic foraminifera, echinoderms, and algae (Fig. 9A) that provide undisputable evidence for derivation from a shallow water carbonate platform rimmed by rudist reefs. Overall, the breccia consists of a mixture of shallow water limestones and angular clasts of greenish, altered volcaniclastic rocks and mainly green and black chert (Fig. 9B), locally up to several meters across (Pszczolkowski, 1994). Quartz grains, microcline, benthic foraminifera, radiolaria test, and micrite are common components of the breccia matrix. The presence of quartz and microcline grains strongly suggests that the breccia has been derived from a continental margin and not from the Cuban volcanic arc as suggested by Takayama et al. (2000). The basal breccia grades upward into a coarse calcirudite, which in turn grades into coarse grainstones capped by fine silt-size grainstone containing planktonic foraminifera. Takayama et al. (2000) found vesicular glass and shocked quartz in the upper part of a correlative mega-bed near Havana (the Penalver Formation). Their biostratigraphic study restricts the age of Penalvar Formation as overlying Late Maastrichtian age strata and underlying Danian strata. The mega bed at Sierra Rosario most likely represents a single depositional event triggered by Chicxulub meteorite impact, as suggested by Pszczolkowski (1994). The seismic tremors resulted in a collapse of the part of the Yucatan outer shelf edge, with submarine avalanches became channelized into debris flows which scoured and eroded the oceanic floor. A reflection seismic profile shot between Campeche Platform and Bahamas (Fig. 9; line SF-15, in Buffler et al., 1984) shows a deep sea channel, almost 10 km wide, where Middle to Upper Cretaceous strata were removed by erosion. The Sierra Rosario breccia contains a high percentage of angular clasts of radiolarite lithologically similar to Albian–Cenomanian radiolarites exposed in Sierra Rosario. Therefore, we conclude that the ‘‘channel’’ may have been scoured by the southeastward-directed Chicxulub debris flow. The limestone breccia at the base of Campeche Escarpment, which was penetrated at Site 536 (Unit 1 of Alvarez et al., 1992), most probably represents a landward-directed edge of one of the debris flows triggered by the impact, which came to rest at the base of the Campeche escarpment.

A different deposit resulting from seismic waves propagation, or by a tsunami wave generated by Chicxulub impact, was recently recognized on the edge of the Blake Plateau (Norris et al., 1999, 2001). Drilling during ODP Leg 171B and seismic evidence recorded slumping of Upper Cretaceous beds on the continental slope. A 10-cm-thick layer of green spherules containing fragments of chalk, limestone, chert, mica, schist, as well as shocked quartz, was penetrated at Site 1049. The upper part of the bed contains an iridium anomaly. The first Paleocene planktonic foraminifera and calcareous nanofossil species were recorded immediately

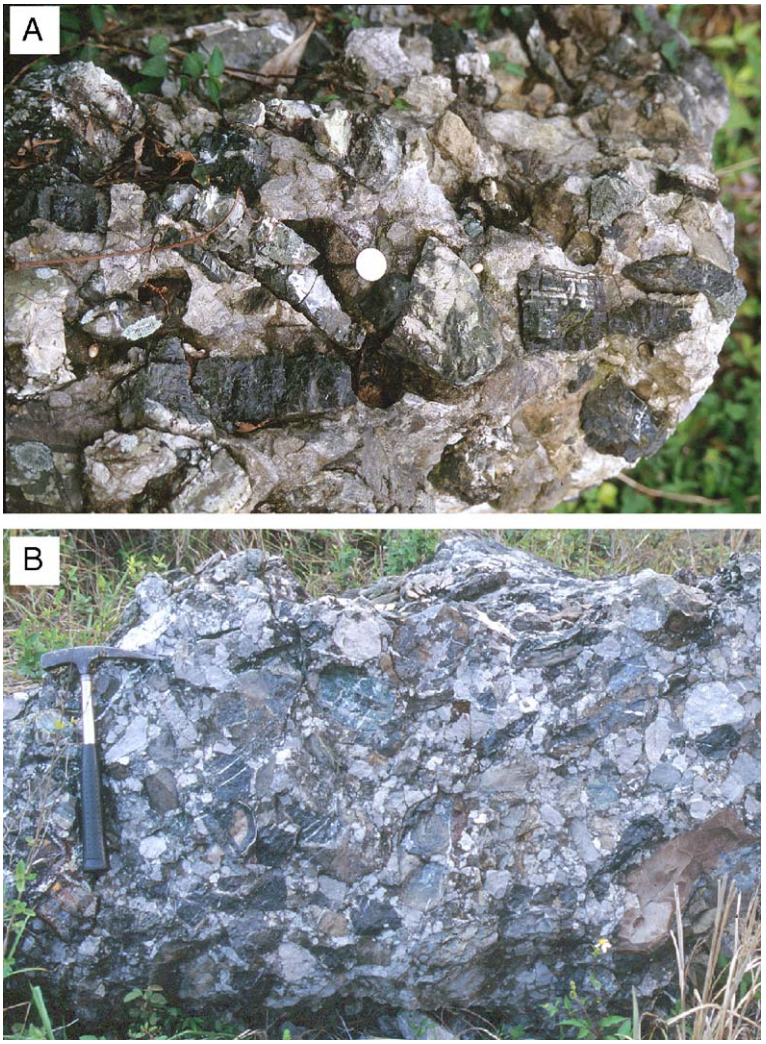

Fig. 9. Composition of *K*/*T* megaturbidite bed from the Los Cayos Member, exposed in Miracielo, western Cuba. Hammer for scale. (A) Close up view of clast-supported breccia. It shows poor sorting, clasts do not show any preferential orientation and are mainly angular. Some shallow-water limestone clasts enclose rudist fragments; some of the chert clasts are thinly laminated. The coin is 2 cm in diameter. (B) Block of the limestone breccia showing angular limestone clasts (gray), black chert clasts, and rare igneous rocks clasts (green).

above the spherule bed (Norris et al., 1999), representing Chicxulub impact ejecta. The slumped beds can be seismically correlated with Horizon A* (Tucholke, 1979), which can be recognized as far as 1000 km east of the eastern North America shelf. This seismic reflector has been correlated with the Crescent Peaks Member (Jansa et al., 1979), which is an olive grey marly chalk in places intercalated with claystones. Its thickness varies from several meters to several tens of meters. The chalk is enclosed within a pelagic reddish clay sequence (the Plantagenat Formation) and was considered to indicate a major drop in the carbon dissolution level (Jansa et al., 1979). However, drilling at Blake Nose showed that the Crescent Peaks chalk is correlative with the *K*/*T* boundary disturbance. Thus, the Crescent Peaks chalk is best interpreted as derived from pelagic carbonate deposited on the eastern North American shelf that was remobilized due to liquefaction by seismic tremors, triggered by the Chicxulub impact. A plume would generate transport of the

carbonate ooze offshore. Turbidite currents could also have been triggered by the same event, as suggested by Norris et al. (1999), transporting fine-grained pelagic carbonate far into the deep basin. A mega-tsunami may have played an important role in the Blake Plateau shelf scouring, opening a deep-water passage from the Yucatan toward the Blake Nose.

5. Conclusions

The physics of impacts into consolidated, well cemented, and crystalline target rocks is known to some extent. In contrast, the knowledge of impacts into successions of wet, unconsolidated sediments covered by a water blanket has not been very much studied. Comparison of two of the best known submarine impact craters, the Montagnais and the Mjølnir craters, allows a more detailed assessment of processes specific to marine environments. Initially, as the water returns to the excavating cavity, where at the time of the impact the initial temperature is in a range of several thousand degrees centigrade, it changes into steam that expels more ejecta. Return water flow into the excavating cavity generates currents that rework and retransport previously ejected material, returning it to the excavated impact crater cavity. As a consequence, the regional distribution of fall-out breccia in marine impacts is generally more restricted than in land impacts and a thicker impact breccia accumulation within the impact crater may result. Resurge gullies are another feature specific to subaqueous craters. Such erosional features result from submarine erosion which bevels off the crater rim, causing lower, more subtle rims or almost complete removal of a rim. In contrast, impacts on land always have well-developed elevated crater rims prior to long-term erosion. In shallow submarine impacts, the top of the central peak is flat as a result of scouring and reworking of impact deposits by waves and shallow currents. This is an additional criterion recognizing neritic impact structures.

Some geochemical (Ir), mineralogical (e.g. shocked quartz, Ni-spinels), and macroscopic (shatter cones) impact markers are common to both subaerial and subaqueous impact craters. However, partial isotropization of quartz and feldspar grains seems to be more frequent in subaqueous than on land impacts.

Among the sedimentological features characteristic of submarine impacts, we include the generation of extensive debris flows and turbidites resulting in the formation of sedimentary sequences with complex architecture and multiple erosion surfaces. This has been documented for the Chicxulub impact, as is the fact that large impacts may result in partial collapse of the outer continental margin. The channelized debris flow from the collapse of the Yucatan continental margin may have traveled for several thousand kilometers, eroding the bathyal ocean floor, and deposited a chaotic mixture of shallow water carbonate and bathyally deposited sedimentary rocks debris in a single, 400 m thick megaturbidite bed, which can be followed for 800 km from western to eastern Cuba. However, the only evidence for the impact origin of these gravity deposits is the presence of various forms of melts and increases in iridium.

Lack of undisputable gigantic tsunami deposits resulting from an impact of a large Chicxulub-type of a bolide outside of Gulf of Mexico indicates that the transfer of energy could be regionally restricted by the bathymetry of the surrounding area, or as result of nonlinearity of waves and the conversion of the coherent energy into turbulence (Strelitz, 1979). A Chicxulub impact-triggered earthquake, perhaps jointly with a mega-tsunami, liquefied pelagic carbonate shelf deposits of the eastern North American margin, with the sediment in suspension being redeposited in the adjacent deep western North Atlantic basin (Norris et al., 1999). Such chalks (the Crescent Peaks Member, Jansa et al., 1979) were previously considered to originate by the change in the CCD.

Ancient marine sedimentary records contain ample amounts of erosion surfaces and disconformities of an unknown origin, some of which could have been caused by a bolide impact-generated mega-tsunami. Meteorites of 30–1000 m in radius strike the Earth every 1000–300,000 years (Shoemaker et al., 1990; Toon et al., 1994; Ward and Asphaug, 2000), and some of them would impact the ocean. However, an asteroid greater than 2 km in diameter would be required to generate a mega-tsunami, presenting hazard throughout the entire Atlantic (Crawford and Mader, 1998).

Our knowledge of marine impacts is not limited because they were rare in the past. It is due to oceanic plate subduction, our insufficient knowledge of de-

tailed ocean bottom morphology and of the criteria for recognizing such events in the ancient rock records.

Acknowledgements

Our presentation has been influenced by discussions of cratering processes with J. Melosh, T. Ahrens, and R. Grieve, which we acknowledge. Brian Petrie provided some data for shallow waves. An early draft of the manuscript was greatly improved by comments of Bruce Simonson, Wylie Poag, Filippos Tsikalas, John Warme, Ray Cas, Keith A.W. Crook, and Frank Thomas. This is Geological Survey of Canada Contribution # 2002184.

References

Abels, A., Plado, J., Pesonen, L.J., Lehtinen, M., 2002. The impact cratering record of Fennoscanida—a close look at the database. In: Plado, J., Pesonen, L.J. (Eds.), Impacts in Precambrian Shields. Springer, Heidelberg, pp. 1–58. 336 pp.

Adette, T., Stinnesbeck, W., Keller, G., 1996. Lithostratigraphic and mineralogic correlations of near-*K*/*T* boundary clastic sediments in Northeastern Mexico: implication for origin and nature of deposition. In: Ryder, G., Fastovsky, D., Gartner, S. (Eds.), The Cretaceous–Tertiary Event and other Catastrophes in Earth History. Geol. Soc. Am. Special Paper, vol. 307, pp. 211–226.

Ahrens, T.J., O'Keefe, J.D., 1983. Impact of an asteroid or comet in the ocean and the extinction of terrestrial life. Proceedings of the 13th Lunar Planetary Conference, Part 2. Journal of Geophysical Research, vol. 88 (supplement), pp. A799–A806.

Albertao, G.A., Martins Jr., P.P., 1996. A possible tsunami deposit at the Cretaceous–Tertiary boundary in Pernambuco, northeastern Brazil. Sedimentary Geology 104, 189–201.

Alvarez, W., Smit, J., Lowrie, W., Asaro, F., Margolis, S.V., Claeys, P., Kastner, M., Hildebrand, A.R., 1992. Proximal impact deposits at the Cretaceous–Tertiary boundary in the Gulf of Mexico: a study of DSDP Leg 77, Sites 536 and 540. Geology 20, 697–700.

Austin Jr., J.A., Schlager, W., Comet, P.A., Droxler, A.W., Eberli, G.P., Fopurcade, E., Freeman, L.R.P., Fulthorpe, C.S., Harwood, G.M., Kuhn, G., m Lavoie, D., Lekie, R.M., Melillo, A.J., Moore, A., Mullins, H.T., Ravenne, C., Sager, W.W., Swart, P.K., Verbeek, J.W., Watkins, D.K., Williams, C.F., Palmer, A., Rose, W.D., Stewart, S.K., 1988. Proceedings of the Ocean Drilling Program, Bahamas, covering Leg 101 of the cruises of the drilling vessel JOIDES Resolution, Miami, Florida to Miami, Florida, sites 626–636. Scientific results, vol. 101. Texas A&M University, Ocean Drilling Program, College Station, TX, USA. 501 pp.

Bahlburg, H., Claeys, P., 1999. Tsunami deposit or not: the problem of interpreting the siliciclastic *K*/*T* sections in Northeastern Mexico. In: Gersonde, R., Deutsch, A. (Eds.), IMPACT Meeting: Oceanic Impacts: Mechanisms and Environmental Perturbations. Kamloth, Bremerhaven, pp. 17–19. Abstracts.

Bazilevskiy, A.T., Kapuskina, V.I., Kolesov, G.M., 1984. The iridium distribution in rocks from terrestrial impact craters. Geochimya 6, 781–790.

Bohor, B.F., 1996. A sediment gravity flow hypothesis for siliciclastic units at the *K*/*T* boundary, Northeastern Mexico. In: Ryder, G., Fastovsky, D., Gartner, S. (Eds.), The Cretaceous–Tertiary Event and other Catastrophes in Earth History. Geol. Soc. Am. Special Paper, vol. 307, pp. 183–196.

Bourgeois, J., Hansen, T.A., Wiberg, P.L., Kauffman, E.G., 1988. A tsunami deposit at the Cretaceous–Tertiary boundary in Texas. Science 241, 567–570.

Bralower, T.J., Paull, Ch.K., Leckie, M.R., 1998. The Cretaceous/Tertiary boundary cocktail: Chicxulub impact triggers margin collapse and extensive sediment gravity flows. Geology 26, 331–334.

Buffler, R.T., Schlager, W., et al., 1984. Initial Reports of the Deep Sea Drilling Project, Leg 77 U.S. Government Printing Office, Washington.

Cita, M.B., Camerlenghi, A., Rimoldi, B., 1996. Deep-sea tsunami deposits in the eastern Mediterranean: new evidence and depositional models. Sedimentary Geology 104, 155–173.

Crawford, D.A., Mader, C., 1998. Modeling asteroid impact and tsunami. Science of Tsunami Hazards 16, 21–30.

Dypvik, H., Attrep Jr., M., 1999. Geochemical signals of the Late Jurassic, marine Mjølnir impact. Meteoritics and Planetary Science 34, 393–406.

Dypvik, H., Ferrel Jr., R.E., 1998. Clay mineral alterations associated with a submarine meteorite impact. Clay Minerals 33, 51–64.

Dypvik, H., Gudlaugsson, S.T., Tsikalas, F., Attrep Jr., M., Ferrell Jr., R.E., Krinsley, D.H., Mørk, A., Faleide, J.I., Nagy, J., 1996. The Mjølnir structure—an impact crater in the Barents Sea. Geology 24, 779–782.

Edwards, A., 1989. Geophysical investigations of potential meteorite impact site offshore Nova Scotia, Canada. Poster, Amer. Assoc. Petrol. Geologists Meeting, Dallas.

Felton, E.A., Crook, K.A.W., 2003. Evaluating the impacts of huge waves on rocky shorelines: an essay review of the book "Tsunami, the Underrated Hazard". Marine Geology 197, 1–12.

French, B.M., 1998. Traces of catastrophe: a handbook of shock-metamorphic effects in terrestrial meteorite impact structures. LPI Contrib., vol. 954. Lunar and Planetary Institute, Houston. 120 pp.

French, B., Koeberl, C., Gilmour, I., Shirey, S.B., Dons, J.A., Naterstad, J., 1997. The Gardnos impact structure, Norway: petrology and geochemistry of target rocks and impactites. Geochimica et Cosmochimica Acta 61, 873–904.

Gault, D.E., Sonett, Ch.P., 1982. Laboratory simulation of pelagic asteroidal impact: atmospheric injection, benthic topography and the surface wave radiation field. In: Silver, L.T., Schultz, P.H. (Eds.), Geological Implications of Impacts of Large Asteroids and Comets on the Earth. Geol. Soc. Amer. Spec-Paper, vol. 190, pp. 69–92.

Gerasimov, M.V., 1999. Mortal Consequences of a Catastrophic Impact: Experimental Evidence. IMPACT Meeting, Workshop on Geological and Biological Evidence for Global Catastrophes, Esperaza/Quillan, France. Abstract, 27.

Gerasimov, M.V., Dikov, Yu.P., Yakovlev, O.I., Wlotzka, F., 1999. Experimental investigation of the role of water in the impact vaporization chemistry. In: Gersonde, R., Deutsch, A. (Eds.), IMPACT Meeting: Oceanic Impacts: Mechanisms and Environmental Perturbations. Kamloth, Bremerhaven, pp. 17–19. Abstracts.

Gersonde, R., Kyte, F.T., Bleil, U., Diekman, B., Flores, J.A., Gohl, K., Grahl, G., Hagen, R., Kuhn, G., Sierro, F.J., Volker, D., Abelmann, A., Bostwick, J.A., 1997. Geological record and reconstruction of the Late Pliocene impact of the Eltanin asteroid in the Southern Ocean. Nature 390, 357–363.

Gersonde, R., Kyte, F.T., Abelmann, A., Bleil, U., Diekman, B., Flores, J.A., Gohl, K., Kuhn, G., Sierro, F.J., 1999. A Late Pliocene asteroid impact into the deep ocean (Bellinghausen Sea)—its documentation and paleoenvironmental implications. IMPACT Meeting: Oceanic Impacts: Mechanisms and Environmental Perturbations. Kamloth, Bremerhaven, pp. 31–33. Abstracts.

Gersonde, R., Deutsch, A., Ivanov, B.A., Kyte, F.T., 2002. Oceanic impacts—a growing field of fundamental science. Deep Sea Research II 49, 951–957.

Glass, B.P., 1986. Late Eocene microtektites and clinopyroxene-bearing spherules. In: Pomerol, Ch., Premoli-Silva, I. (Eds.), Terminal Eocene Events. Elsevier Science Publishers, Amsterdam, pp. 395–401.

Glass, B.P., Koeberl, C., 1999. Ocean drilling project hole 689B. Spherules and upper Eocene microtectites and clinopyroxene-bearing spherule strewn fields. Meteoritics and Planetary Science 34, 197–208.

Glikson, A.Y., 1999. Oceanic mega impacts and crustal evolution. Geology 27, 387–390.

Goff, J., Chaque-Goff, C., Nichol, S., 2001. Paleotsunami deposits: a New Zealand perspective. Sedimentary Geology 143, 1–6.

Gostin, V.A., Therriault, A.M., 1997. Tookoonooka, a large buried Early Cretaceous impact structure in the Eromanga Basin of southwestern Queensland, Australia. Meteoritics and Planetary Science 32, 593–599.

Grajales-Nishimyra, J.M., Cedillo-Pardo, E., Rosales-Dominguez, C., Moran-Zenteno, D.J., Alvarez, W., Claeys, P., Ruiz-Morales, J.G., Garcia-Herdandez, J.G., Padilla-Avila, P., Sanches-Rios, A., 2000. Chicxulub impact: the origin of reservoir and seal facies in the southeastern Mexico oil fields. Geology 28, 307–310.

Grieve, R.A.F., 1998. Extraterrestrial impacts on earth: the evidence and consequences. In: Grady, M.M., Hutchinson, R., McGall, G.J.M., Rothery, D.A. (Eds.), Meteorites: Flux with Time and Impact Effects. Geol. Soc. London Spec. Publ., vol. 140, pp. 105–131.

Grieve, R.A.F., Robertson, P.B., Dence, M.R., 1981. Constraints on the formation of ring impact structures, based on terrestrial data. In: Schultz, P.H., Merrill, R.B. (Eds.), Multi-ring Basins: Proceedings of the 12th Lunar and Planetary Science Conference, vol. 12A, pp. 37–57.

Grieve, R.A.F., James, R., Smit, J., Terriault, A., 1995. The record of terrestrial impact cratering. GSA Today 5 (10), 193–196.

Gudlaugsson, S.T., 1993. Large impact crater in the Barents Sea. Geology 21, 291–294.

Hale, W., Head, J.W., 1979. Central peaks in lunar craters: morphology and morphometry. Proc. 10th. Lunar Planet. Sci., pp. 2623–2633.

Hartley, A., Howell, J., Mather, A.E., Chong, G., 2001. A possible Plio-Pleistocene tsunami deposit, Hornitos, northern Chile. Revista Geologica de Chile 28 (1), 117–125.

Hildebrand, A.R., Boynton, W.V., 1990. Proximal Cretaceous–Tertiary boundary impact deposits in the Caribbean. Science 248, 843–847.

Hildebrand, A.R., Penfield, G.T., Kring, D.A., Pilkington, M., Camargo, A., Jacobsen, S.B., Boynton, W.V., 1991. Chicxulub crater: a possible Cretaceous/Tertiary boundary impact crater on the Yucatan Peninsula, Mexico. Geology Review 36, 105–151.

Ivanov, B.A., 1999. Impact ejecta deposition around impact craters: interplanetary comparison and models. IMPACT Meeting, Workshop on Geological and Biological Evidence for Global Catastrophes, Esperaza/Quillan, France. Abstract, 42.

Jansa, L.F., 1993. Cometary impacts into ocean: their recognition and threshold constraint for biological extinctions. Palaeogeography Palaeochimica Palaeoecology 104, 271–286.

Jansa, L.F., Pe-Piper, G., 1987. Identification of an underwater extraterrestrial impact crater. Nature 327, 612–614.

Jansa, L.F., Enos, P., Tucholke, B.E., Gradstein, F.M., Sheridan, R.E., 1979. Mesozoic–Cenozoic sedimentary formations of the North American Basin; Western North Atlantic. In: Talwani, M., Hay, W., Ryan, W.B.F. (Eds.), Deep Drilling Results in the Atlantic Ocean: Continental Margins and Paleoenvironment. American Geophysical Union, Maurice Ewing Series, vol. 3, pp. 1–57.

Jansa, L.F., Pe-Piper, G., Robertson, B., Friedenreich, O., 1989. Montagnais: a submarine impact structure on the Scotian Shelf, eastern Canada. Geological Society of America Bulletin 101, 450–463.

Kirschner, C.E., Grantz, A., Mullen, M.N., 1992. Impact origin of the Avak structure, Arctic Alaska, and Genesis of the Barrow Gas Fields. American Association of Petroleum Geologists Bulletin 76, 651–679.

Koeberl, C., 1993. Tektite origin by hypervelocity asteroidal or cometary impact: target rocks, source craters, and mechanism. In: Dressler, B.O., Grieve, R.A.F., Sharpton, V.L. (Eds.), Large Meteorite Impacts and Planetary Evolution, Sudbury, 1992. Geological Society of America, Special Paper, vol. 293, pp. 133–151.

Koeberl, C., Reimold, W.U., 1999. Comment. Geology 27, 281–282.

Koeberl, C., Sharpton, V.L., Murali, A.V., Bruke, K., 1990. Kara and Ust-Kara impact structures (USSR) and their relevance to the *K*/*T* boundary event. Geology 18, 50–53.

Koeberl, C., Reimold, W.U., Boer, R.H., 1993. Geochemistry and mineralogy of Early Archaen spherule beds Barberton Mountain Land, South Africa: evidence for origin by impact doubtful. Earth and Planetary Science Letters 119, 441–452.

Kyte, F., 2002. Unmelted meteoritic debris collected from Eltanin ejecta in Polarstern cores from expedition ANT XII/4. Deep Sea Research II 49, 1063–1071.

Kyte, F., Zhou, Z., Wasson, J.T., 1981. High noble metal concentrations in a Late Pliocene sediment. Nature 292, 417–420.

Kyte, F., Botswick, J.A., Zhou, L., 1996. The Cretaceous–Tertiary boundary on the Pacific Plate; composition and distribution of impact debris. In: Ryder, G., Fastovsky, D., Gartner, S. (Eds.), The Cretaceous–Tertiary Event and Other Catastrophes in Earth History. Geol. Soc. Am., Spec. Paper, vol. 307, pp. 389–401.

Lindstrøm, M., Strukell, E.F.F., 1992. Geology of the Early Paleozoic Lockne impact structure, Central Sweden. Tectonophysics 216, 169–185.

Lindstrøm, M., Flodèn, T., Grahn, Y., Kathol, B., 1994. Post impact deposits in Tvären, a marine Ordovician crater south of Stockholm, Sweden. Geological Magazine 131, 91–103.

Lindstrøm, M., Strukell, E.F.F., Tørnberg, R., Ormø, J., 1996. The marine impact crater at Lockne, central Sweden. Geologiske Føreningen Førhdl 118, 193–206.

Masaitis, V.L., 1994. Impactites from Popigai Crater. In: Dressler, B.O., Grieve, R.A.F., Sharpton, V.L. (Eds.), Large Meteorite Impacts and Planetary Evolution. Geol. Soc. Am. Paper, vol. 293, pp. 153–162.

Masaitis, V.L., 1999. Impact structures of northeastern Eurasia: the territories of Russia and adjacent countries. Meteoritics and Planetary Sciences 34, 691–711.

Masaitis, V.L., 2002. The Middle Devonian Kaluga impact event (Russia): new interpretation of marine setting. Deep Sea Research II 6, 1157–1169.

Masaitis, V.L., Mashchak, M.S., 1982. The shower of cosmic bodies falls 65 my ago? The Lunar and Planetary Science 13, 469–470.

Masaitis, V.L., Nazarov, M.A., Badyukov, D.D., Ivanova, B.A., 1991. Impact events at the Cretaceous–Tertiary boundary. International Geology Review 33, 663–679.

Mashchak, M.S., 1990a. Geologic setting in Kara and Ust'-Kara at the time of formation of the impact craters (Geologicheskaya obstnovka vremeni obrazovaniya impaktnykh kraterov na Pay-Khoye). In: Masaytis, V.L. (Ed.), Impaktnyye kretery na rubezne mzozoya i kaynozoya (Impact Craters of the Mesozoic–Cenozoic Boundary). Nauka Press, Leningrad, pp. 24–37.

Mashchak, M.S., 1990b. Morphology and structure of the Kara and Ust'-Kara astroblems (Morfologiya i struktura Karkoy i Ust'-Karskoy astroblem). In: Masaytis, V.L. (Ed.), Impaktnyye kretery na rubezne mzozoya i kaynozoya (Impact Craters of the Mesozoic–Cenozoic Boundary). Nauka Press, Leningrad, pp. 37–55.

Melosh, H.J., 1989. Impact Cratering. A Geologic Process. Oxford Univ. Press, Oxford, UK. 245 pp.

Moore, J.C., Klaus, A., Bangs, N.L., Bekins, B., Brueckmann, W., Buecker, C.J., Erikson, S.N., Hansen, O., Horton, T., Ireland, P., Major, C.O., Moore, G.P., Peacock, S., Saito, S., Screaton, E.J., Shimeld, J.W., Stauffer, P.H., Taymaz, T., Teas, P.A., Tokunaga, T., Baez, L.A., Kapitan, W.E., 1998. Site 1048. Proceedings of the Ocean Drilling Program, Part A. Initial reports. 171 A. College Station, TX, US.

Mørk, A., Dypvik, H., Smelror, M., 2000. The Mjølnir Impact Core from the Barents Sea—Exhibition of Some Key Parts of the Core, 24. Nordic Winter meeting, Trondheim 2000. Proceedings, p. 124.

Nordyke, M.D., 1977. Nuclear cratering experiments; United States and Soviet Union. In: Roddy, D.J., Pepin, R.O., Merrill, R.B. (Eds.), Impact and Explosion Cratering; Planetary and Terrestrial Implications. Proceedings of the Symposium on Planetary Cratering Mechanics. Pergamon, New York, USA, pp. 103–124.

Norris, R.D., Huber, B.T., Self-Trail, J., 1999. Synchroneity of the *K–T* oceanic mass extinction and meteorite impact: Blake Nose, western North Atlantic. Geology 27, 419–422.

Norris, R.D., Klaus, A., Kroon, D., 2001. Mid-Eocene deep water, the Late Paleocene thermal maximum and continental slope mass wasting during the Cretaceous–Paleogene impact. In: Kroon, D., Norris, R.D., Klaus, A. (Eds.), Western North Atlantic Paleogene and Cretaceous Paleoceanography. Geological Society London, Spec. Publications, vol. 183, pp. 23–48.

Oberbeck, V.R., Marshall, J.R., Aggarwal, H., 1993. Impacts, tillites, and the breakup of Gondwanaland. Journal of Geology 101, 1–19.

Ocampo, A., Pope, K.O., Fischer, A.G., 1996. Ejecta blanket deposits of the Chicxulub Crater from Albion Island, Belize. In: Ryder, G., Fastovsky, D., Gartner, S. (Eds.), The Cretaceous–Tertiary Event and other Catastrophes in Earth History. Geol. Soc. Am. Special Paper, vol. 307, pp. 75–88.

O'Keefe, J.D., Ahrens, T.J., 1982. The interaction of the Cretaceous/Tertiary extinction bolide with the atmosphere, ocean and solid Earth. Geological Society of America Special Paper 190, 103–120.

Ormø, J., 1998. Impact cratering at sea. Medd. Stockh. Univ. Inst. før Geol. Och. Geochim., 300 pp. Ph.D thesis Stockholm University, 1998.

Ormø, J., Lindstrøm, M., 1999. Geological characteristics of marine target craters. In: Gersonde, R., Deutsch, A. (Eds.), Oceanic Impacts, Mechanisms and Environmental Perturbations, ESF-IMPACT Workshop. Berichte zur Polarforschung, vol. 343, pp. 70–74.

Ormø, J., Lindstrøm, M., 2000. When a cosmic impact strikes the sea bed. Geological Magazine 137, 67–80.

Ormø, J., Miyamoto, H., 2002. Computer modelling of the water resurge at a marine impact: the Lockne crater, Sweden. Deep-Sea Research II 49, 983–994.

Pickering, K.T., Soh, W., Taira, A., 1991. Scale of tsunami-generated sedimentary structures in deep water. Journal of the Geological Society, London 148, 211–214.

Pike, R.J., 1985. Some morphologic systematics of complex impact structures. Meteoritics 20, 49–68.

Pilkington, M., Jansa, L.F., Grieve, R.A.F., 1995. Geophysical studies of the Montagnais impact crater, Canada. Meteoritics 30, 446–450.

Plado, J., Pesonen, L., Elo, S., Puura, V., Suuroja, K., 1996. Geophysical research on the Kärdla impact structure, Hiiumaa Island, Estonia. Meteoritics and Planetary Science 31, 289–298.

Poag, C.W., 1996. Structural outer rim of Chesapeake Bay impact crater: seismic and bore hole evidence. Meteoritics and Planetary Science 31, 218–226.

Poag, C.W., 1997. The Cheasapeak Bay bolide impact: a convulsive

event in Atlantic coastal plain evolutions. Sedimentary Geology 108, 45–90.

Poag, C.W., Powars, D.S., Poppe, L.J., Mixon, R.B., 1994. Meteorid mahem in Ole Virginny: source of the North American tektites threwn field. Geology 22, 691–694.

Poag, C.W., Hutchinson, D.R., Colman, S.M., Lee, M.Y., 1999. Seismic expression of the Chesapeake Bay impact crater, structural and morphologic refinements based on new seismic data. In: Dressler, B.O., Sharpton, V.L. (Eds.), Large Meteorite Impacts and Planetary Evolution II. Geol. Soc. Am., vol. 339, pp. 149–164.

Postma, H., 1967. Sediment transport and sedimentation in the estuary environment. In: Lauff, G.H. (Ed.), Estuaries, Pub., vol. 83. American Association for Advancement of Science, Washington, DC, pp. 158–179.

Pszczolkowski, A., 1986. Megacapas del Maestrichtiano en Cuba occidental y central. Bulletin of the Polish Academy of Sciences. Earth Science 34, 81–94.

Pszczolkowski, A., 1994. Lithostratigraphy of Mesozoic and Paleogene rocks of Sierra del Rosario, Western Cuba. Studia Geologica Polonica 105, 39–62.

Puura, V., Suuroja, K., 1992. Ordovican impact crater at Kärdla, Hiiumaa, Estonia. Tectonophysics 216, 143–156.

Rocchia, R., Robin, E., Froget, L., Gayraud, J., 1996. Stratigraphic distribution of extraterrestrial markers at the Cretaceous–Tertiary boundary in the Gulf of Mexico area: implications for the temporal complexity of the event. In: Ryder, G., Fastovsky, D., Gartner, S. (Eds.), The Cretaceous–Tertiary Event and other Catastrophes in Earth History. Geol. Soc. Am. Special Paper, vol. 307, pp. 279–286.

Roddy, D.J., Schuster, S.H., Rosenblatt, M., Grant, L.B., Hassing, P.J., Kreyenhagen, K.N., 1987. Computer simulations of large asteroid impacts into oceanic continental sites; Preliminary results on atmospheric cratering and ejecta dynamics. International Journal of Impact Engineering 5, 525–541.

Rondot, J., 1994. Recognition of eroded astroblems. Earth-Science Reviews 35, 331–365.

Schlager, W., Buffler, R.T., Angstadt, D., Phair, R., 1984. Geologic history of the southeastern Gulf of Mexico. Initial Reports of the Deep Sea Drilling Program, Leg 77. U.S. Government Printing Office, Washington, pp. 715–738.

Selivanovskaya, T.V., Mashchak, M.S., Masayitis, V.L., 1990. Impact breccias and impactites of the Kara and Ust'-Kara Astroblems (Impaktnyye brekchii i impaktity Karakoy i Ust'-Karskoy astroblem). In: Masaytis, V.L. (Ed.), Impaktnyye kretery na rubezne mzozoya i kaynozoya (Impact Craters of the Mesozoic–Cenozoic Boundary, 1990). Nauka Press, Leningrad, pp. 55–96.

Sharpton, V.L., Grieve, R.A.F., 1990. Meteorite impact, cryptoexplosion, and shock metamorphism: a perspective on the evidence at the *K*/*T* boundary. Geological Society of America, Special Paper 247, pp. 301–318.

Sharpton, V.L., Marin, L.E., Carney, J.L., Lee, S., Ryder, G., Schuraytz, B.C., Sikora, P., Spudis, P.D., 1996. A model of the Chicxulub impact basin based on evaluation of geophysical data, well logs and drill core samples. In: Ryder, G., Fastovsky, D., Gartner, S. (Eds.), The Cretaceous–Tertiary Event and other Catastrophes in Earth History: Boulder, Colorado. Geological Soc. Am. Special Paper, vol. 307, pp. 55–74.

Shaw, H.F., Wasserburg, G.J., 1982. Age and provenance of the target materials for tektites and possible impactites as inferred from Sm–Nd and Rb–Sr systematics. Earth and Planetary Science Letters 60, 155–177.

Shiki, T., Cita, M.B., Gorsline, D.S., 2000. Sedimentary features of seismites, seismo-turbidites and tsunamiites—an introduction. Sedimentary Geology 135, VII–IX.

Shoemaker, E.M., Wolfe, R.F., Shoemaker, C.S., 1990. Asteroid and comet flux in the neighborhood of Earth. In: Sharpton, V.L., Ward, P.D. (Eds.), Global Catastrophes in Earth History. Geol. Soc. Am. Special Paper, vol. 247, pp. 155–170.

Sigurdsson, H., D'Hondt, S., Arthur, M.A., Bralower, T.J., Zachos, J.C., van Fossen, M., Channell, J.E.T., 1991. Glass from the Cretaceous/Tertiary boundary in Haiti. Nature 239, 482–487.

Simonson, B.M., 1992. Geological evidence for a strewn field of impact spherules in the Early Precambrian Hamersley Basin of Western Australia. Geological Society of America Bulletin 104, 829–839.

Simonson, B.M., Harnik, P., 2000. Have distal impact ejecta changed through geologic time? Geology 28, 975–978.

Simonson, B.M., Hassler, S.W., 1997. Revised correlations in the Early Precambrian Hamersley Basin based on a horizon of resedimented impact spherules. Australian Journal of Earth Sciences 44, 37–48.

Simonson, B.M., Davies, D., Wallace, M., Reeves, S., Hassler, S.W., 1998. Iridium anomaly but no shocked quartz from Late Archean microkrystite layer: Oceanic impact ejecta? Geology 26, 195–198.

Smelror, M., Kelley, S., Dypvik, H., Mørk, A., Nagy, J., Tsikalas, F., 2001. Mjølnir (Barents Sea) meteorite impact ejecta offers a Boreal Jurassic–Cretaceous boundary marker. Newsletters in Stratigraphy 38, 129–140.

Smit, J., 1999a. Ejecta deposits of the Chicxulub impact. Impact meeting: Oceanic Impacts: Mechanisms and Environmental Perturbations. Kamloth, Bremerhaven, pp. 84–85. Abstracts.

Smit, J., 1999b. The global stratigraphy of the Cretaceous–Tertiary boundary impact ejecta. Annual Review of Earth and Planetary Sciences 27, 75–113.

Smit, J., Montanari, A., Swinburne, N.H.M., Hildebrand, A.R., Margoli, S.V., Claeys, P., Lowrie, W., Asaro, F., 1992. Tektite-bearing, deep-water clastic unit at the Cretaceous–Tertiary boundary in northeastern Mexico. Geology 20, 99–103.

Smit, J., Roep, Th.B., Alvarez, W., Montanari, A., Claeys, P., Grajales-Nishimura, J.M., Bermudez, J., 1996. Coarse-grained, clastic sandstone complex at the *K*/*T* boundary around the gulf of Mexico: deposition by tsunami waves induced by the Chicxulub impact? In: Ryder, G., Fastovsky, D., Gartner, S. (Eds.), The Cretaceous–Tertiary Event and other Catastrophes in Earth History. Geol. Soc. Am. Special Paper, vol. 307, pp. 151–182.

Sonett, Ch.P., Pearce, S.J., Gault, D.E., 1991. The oceanic impact of large objects. Advances in Space Research 11, 77–86.

Stinnesbeck, W., Keller, G., 1996. K/T boundary coarse-grained siliciclastic deposits in Northeastern Mexico and Northeastern Brazil: evidence for Mega-Tsunami or Sea-Level changes. In: Ryder, G., Fastovsky, D., Gartner, S. (Eds.), The Cretaceous–

Tertiary Event and other Catastrophes in Earth History. Geol. Soc. Am. Special Paper, vol. 307, pp. 197–210.

Støffler, D., Langenhorst, F., 1994. Shock metamorphism of quartz in nature and experiment: I. Basic observation and theory. Meteoritics 29, 155–181.

Støffler, D., Ewald, U., Ostertag, R., Reimold, W.-U., 1977. Research drilling Nordlingen 1973 (Ries): composition and texture of polymictic impact breccias. Geologica Bavarica 75, 163–189.

Strelitz, R., 1979. Meteorite impact in the ocean. Proceed. 10th-. Lunar Planet Conf., 2799–2813.

Sturkell, E.F.F., 1998. Resurge morphology of the marine Lockne impact crater, Jämtland, central Sweden. Geological Magazine 135, 121–127.

Sturkell, E.F.F., Ormø, J., 1997. Impact-related clastic injections in the marine Ordovician Lockne impact structure, Central Sweden. Sedimentology 44, 793–804.

Sturkell, E.F.F., Ormø, J., 1998. Magnetometry of the marine, Ordovician Locke impact structure, Jämtland, Sweden. Journal of Applied Geophysics 38, 195–207.

Suuroja, K., Suuroja, S., in press. Neugrund structure—the newly discovered Early Cambrian impact crater at the entrance of the Gulf of Finland, Estonia. In: Dypvik, H., Burchell, M., Claeys, P. (Eds.), Cratering in Marine Environments and on Ice. Impact studies, vol. 5. Springer, Heidelberg, Germany, pp. 75–95.

Suuroja, K., Suuroja, S., All, T., Flodèn, T., 2001. Kärdla (Hiiuma Island, Estonia)—the buried and well-preserved Ordovician marine impact structure. Deep Sea Research, Part II 46, 1121–1144.

Takayama, H., Tada, R., Matsui, T., Iturralde-Vinent, M.A., Oji, T., Tajika, E., Kiyokawa, S., Garcia, D., Okada, H., Hasegawa, T., Toyoda, K., 2000. Origin of the Penalver Formation in northwestern Cuba and its relation to *K*/*T* boundary impact event. Sedimentary Geology 135, 295–320.

Toon, O.B., Zahnle, K., Turco, R.P., Covey, C., 1994. Environmental perturbations caused by asteroid impacts. In: Gehrels, T. (Ed.), Hazards Due to Comets and Asteroids. Univ. of Arizona Press, Tucson, AZ, USA, pp. 791–826.

Tørnberg, R., 1999. Component analysis of the resurge deposits in the marine lockne and Tvären impact structures. Distribution of shock metamorphism in the marine Lockne and Tvären impact structures. In: Gersonde, R., Deutsch, A. (Eds.), IMPACT Meeting: Oceanic Impacts: Mechanisms and Environmental Perturbations. Kamloth, Bremerhaven, pp. 92–94. Abstracts.

Tsikalas, F., Faleide, J.I., in press. Near field erosional features at the Mjølnir impact Crater: the role of marine sedimentary target. In: Dypvik, H., Burchell, M., Claeys, P. (Eds.), Cratering in Marine Environments and on Ice. Impact studies, vol. 5. Springer, Heidelberg, Germany, pp. 40–55.

Tsikalas, F., Gudlaugsson, S.T., Faleide, J.I., 1998a. Collapse, infilling and postimpact deformation at the Mjølnir impact structure, Barents Sea. Geological Society of America Bulletin 110, 537–552.

Tsikalas, F., Gudlaugsson, S.T., Faleide, J.I., 1998b. The anatomy of a buried complex impact structure: the Mjølnir Structure, Barents Sea. Journal of Geophysical Research 103, 30.469–30.483.

Tsikalas, F., Gudlaugsson, S.T., Eldholm, O., Faleide, J.I., 1998a. Integrated geophysical analyses supporting the impact origin of the Mjølnir Structure, Barents Sea. Tectonophysics 289, 257–280.

Tsikalas, F., Gudlaugsson, S.T., Faleide, J.I., Eldholm, O., 1999. Mjølnir structure, Barents Sea: a marine impact crater laboratory. In: Dressler, B.O., Sharpton, V.L. (Eds.), Large Meteorite Impacts and Planetary Evolution; II. Geol. Soc. Amer. Spec. Paper, vol. 339, pp. 193–204.

Tsikalas, F., Gudlaugsson, S.T., Faleide, J.I., Eldholm, O., 2002. The Mjølnir marine impact crater porosity anomaly. Deep-Sea Research II 49, 1103–1120.

Tucholke, B.E., 1979. Relationship between acoustic stratigraphy and lithostratigraphy in the western north Atlantic Basin. In: Tucholke, B.E., Vogt, P.R., et al., (Eds.), Initial Reports of the Deep Sea Drilling Project, vol. 43. US Government Printing Office, Washington, pp. 827–846.

van der Bergh, S., 1989. Life and death in the inner solar system. Publications of the Astronomical Society of the Pacific 101, 500–509.

von Dalwigk, I., Ormø, J., 1999. Formation of resurge gullies at impact at sea: the Lockne Crater Sweden. In: Gersonde, R., Deutsch, A. (Eds.), IMPACT Meeting: Oceanic Impacts: Mechanisms and Environmental Perturbations. Kamloth, Bremerhaven, pp. 22–23. Abstracts.

Ward, S.N., Asphaug, E., 2000. Asteroid impact tsunami: a probabilistic hazard assessment. Icarus 145, 64–78.

Ward, S.N., Asphaug, E., 2002. Impact tsunami—Eltanin. Deep-Sea Research II 49, 1073–1080.

Ward, W.C., Keller, G., Stinnesbeck, W., Adatte, T., 1995. Yucatan subsurface stratigraphy; implications and constraints for the Chicxulub impact. Geology 23, 873–876.

Warme, J.A., Kuehner, H.-Ch., 1998. Anatomy of an anomaly: the Devonian catastrophic Alamo impact breccia of southern Nevada. International Geology Review 40, 189–216.

Warme, J.E., Sandberg, Ch.A., 1995. The catastrophic Alamo breccia of southern Nevada: Record of a Late Devonian extraterrestrial impact. Courier Forschungs, Senckenberg 188, 31–57.

Whitehead, J., 2002. Earth Impact Database. PASSC, Univ. of New Brunswick. http://www.unb.ca/passc/ImpactDatabase/images.html.

Wilshire, H.G., Offield, T.W., Howard, K.A., Cummings, D., 1972. Geology of the Sierra Madera cryptoexplosion structure, Pecos County, Texas. U.S. Geological Survey Professional Paper, H1–H42.

Yancey, T.E., 1997. Tsunamites and bolide impact; Cretaceous–Tertiary boundary deposits, northern shelf of the Gulf of Mexico. Geol. Soc. Am., Annual meeting, Salt Lake City, UT, 20–23 October, Abstracts with programs, 29, 6.

Zakharov, V.A., Lapukhov, A.S., Shenfil, O.V., 1993. Iridium anomaly at the Jurassic–Cretaceous boundary in Northern Siberia. Russian Journal of Geology and Geophysics 34, 83–90.